

Parallel Operation of DC-AC Inverters for Microgrid Application



By

Muhammad Hassan Shah

NUST00000170355MSEE10035

Supervisor

Dr. Sajjad Haider Zaidi

Department of Electronics and Power Engineering

Pakistan Navy Engineering College(PNEC)

National University of Sciences and Technology (NUST)

Islamabad, Pakistan

May 2020

Parallel Operation of DC-AC Inverters for Microgrid Application

By

Muhammad Hassan Shah

NUST00000170355MSEE10035

Supervisor

Dr. Sajjad Haider Zaidi

This thesis is presented for qualifying MS degree
in Electrical(Control) Engineering
Department of Electronics and Power Engineering
Pakistan Navy Engineering College(PNEC)
National University of Sciences and Technology (NUST)
Islamabad, Pakistan
May 2020

Declaration

I, *Muhammad Hassan Shah* declare that this thesis titled “Parallel Operation of DC-AC Inverters for Microgrid Application” and the work presented in it are my own and has been generated by me as a result of my own original research.

I confirm that:

1. This work was done wholly or mainly while in candidature for a Master of Science degree at NUST
2. Where any part of this thesis has previously been submitted for a degree or any other qualification at NUST or any other institution, this has been clearly stated
3. Where I have consulted the published work of others, this is always clearly attributed
4. Where I have quoted from the work of others, the source is always given. With the exception of such quotations, this thesis is entirely my own work
5. I have acknowledged all main sources of help
6. Where the thesis is based on work done by myself jointly with others, I have made clear exactly what was done by others and what I have contributed myself

Muhammad Hassan Shah,
NUST00000170355MSEE10035

Copyright Notice

- Copyright in text of this thesis rests with the student author. Copies (by any process) either in full, or of extracts, may be made only in accordance with instructions given by the author and lodged in the Library of PNEC, NUST. Details may be obtained by the Librarian. This page must form part of any such copies made. Further copies (by any process) may not be made without the permission (in writing) of the author.
- The ownership of any intellectual property rights which may be described in this thesis is vested in PNEC, NUST, subject to any prior agreement to the contrary, and may not be made available for use by third parties without the written permission of PNEC, which will prescribe the terms and conditions of any such agreement.
- Further information on the conditions under which disclosures and exploitation may take place is available from the Library of PNEC, NUST, Karachi.

This thesis is dedicated to *my beloved parents*

Abstract

The energy trading among prosumers (producer and consumer) is a new trend where people can generate their own energy from Renewable Energy Sources (RESs) and share it with each other locally. This forms a local micro grid that can work without connection from traditional grid. A microgrid is helpful in cutting cost in various aspects including transmission and distribution. It also serves as a backup in case of emergencies. And also give opportunity to such power resources that are unreliable or too small for traditional grid use.

A design a strategy is proposed in which DC to AC power sources are operated in parallel in a way that power is shared between them maintaining regulation and stability of voltage and frequency. This could help in energy trading in which every home that is connect to the micro grid with DC to AC converters will be able to share the amount of power according to their capacity.

Thesis begin with the investigation of switching gate drive algorithms that are traditionally used with three phase inverters, and introduces a method of space-vector pulse-width-modulation (SVPWM) in order to get reduced total harmonic distortion.

In the second step synchronous rotating frame model of single phase inverter is discussed. Link between the voltage and phase components of phase signal is reviewed and a new transformation is discussed that used voltage and current values as a reference in the park transformation stages. The line frequency components that are time variant are transformed into time invariant signals that helped in the reduction of computational cost in the controller and eradicating the ripples.

In the end, approach for active and reactive power sharing is discussed which demonstrated the droop control properties are inherited in the control that is designed for inverter. MATLAB (Simulink) environment was used to demonstrate the efficacy of

proposed techniques in the thesis.

Keywords: *DC-AC Inverter, Single Phase, SVPWM, Park Transform, Load Sharing, MATLAB*

Acknowledgments

I am highly thankful to Allah Almighty for providing me such great opportunity to pursue my research work. I would like to thank my supervisor Capt. Dr. Syed Sajjad Haider Zaidi PN, his patience, motivation, enthusiasm and continuous support kept me on track helped me in completing my research. I am also indebted to the GEC committee for their kind support and professional help. I would like to extend special thanks to all the teachers who taught me during my coursework. I am obliged to my family and friends for supporting me throughout this degree. I am also grateful to National University of Science and Technology (NUST) for providing such a pleasant environment and facilities to complete this research.

Contents

1	Introduction	1
1.1	Motivation	1
1.2	Problem Statement and Proposed Solution on the Inverter Side	2
1.3	Thesis structure	4
2	Literature Review and Design Considerations	5
2.1	Introduction	5
2.2	Standard Permits for Grid Connected Inverter System	5
2.3	Voltage Source Inverter: Structure and Operation	6
2.3.1	Single Phase Inverter	6
2.3.2	Modulation Strategy	8
2.3.3	Filetrs	8
2.4	Methods for Inverter Current Control	10
2.4.1	Linear Regulator Based Method	10
2.4.2	Hysteresis Control Method	12
2.4.3	Proportional-Resonant Current Controller	12
2.4.4	Synchronous Rotating Frame Controller	13
2.5	Decentralized Power Supply	13
2.6	LCL Filter Design Consideration	14
3	Space Vector Pulse Width Modulation	19

CONTENTS

3.1	Introduction	19
3.2	General Description of Pulse Width Modulation Techniques	20
3.3	General PWM Classification	21
3.4	Hysteresis Current Controllers	21
3.5	Sinusoidal PWM	22
3.6	SVPWM Technique	24
3.7	Space Vector Concept	24
3.8	The Basic Principle of SVPWM	25
3.9	Software Implementation of Single-Phase SVPWM	26
3.9.1	Boundary and Separation Planes	27
3.9.2	Switching Sequences	27
3.9.3	Time Duration	28
3.9.4	Bipolar SVPWM	28
3.10	Simulation	29
4	Theoretical Aspects of Stationary and Synchronous Rotating Frame	35
4.1	Introduction	35
4.2	Synchronous and Reference Frames in Literature	36
4.3	Synchronous Frame Transformation in Three-Phase System	38
4.4	Rotating Reference Frame Control Structure in Three-Phase Systems	40
4.5	Literature Review For Single-Phase Inverters Employing The Synchronous Rotating Frame Controller	43
4.6	Summary	45
5	Single Phase Inverter Modeling Based on Synchronous Rotating Frame	46
5.1	Introduction	46
5.2	Single Phase Inverter Model	47
5.3	Use of the Imaginary Orthogonal Phase in Single-Phase Systems	48

5.4	Modelling of the Single-Phase Inverter in Stationary and Rotating Reference Frames	49
5.4.1	Single-Phase Inverter Model in Stationary Reference Frame	49
5.4.2	Single-Phase Inverter Model in Rotating Reference Frame	53
5.5	Double Feedback Loop Control Strategy	55
5.6	Grid-tied Inverter Mode	56
5.7	Simulation and Results	58
5.8	Summary	61
6	Drop Control in Synchronous Solid-State Converter	64
6.1	Introduction	64
6.2	Power Network Description	65
6.3	Decentralized Power Management Concept	66
6.4	Impact of Decentralized Distributed Generation on the Network	67
6.5	Drop Function Methodology in Literature	68
6.6	Simulation and Results	73
7	Conclusion and Future Work	76
7.1	Conclusion	76
7.2	Summary	76
7.3	Future Work	78
	References	80

List of Figures

2.1	Single Phase Full Bridge Inverter.	6
2.2	Filter Configuration Circuits.	9
2.3	Carrier-based current control method.	11
2.4	Carrier-based controls scheme with sine transfer function.	11
2.5	Hysteresis current controller scheme.	12
2.6	LCL filter design algorithm.	16
2.7	LCL filter bode plot.	18
3.1	Unipolar PWM and Bipolar PWM.	21
3.2	Hysteresis current controller PWM.	22
3.3	Sinusoidal PWM generation.	23
3.4	Output vector direction of single-phase inverter.	26
3.5	Single-phase inverter vector sequence.	28
3.6	Single-phase Bipolar SVPWM flowchart.	29
3.7	Block diagram of single phase SVPWM generator.	30
3.8	Sector selection.	30
3.9	SVPWM Sector 1.	31
3.10	SVPWM Sector 2.	31
3.11	SVPWM generating gate signal.	32
3.12	Full bridge single phase inverter with LCL filter.	32
3.13	Generated SVPWM gating signal.	33

LIST OF FIGURES

3.14	Output Voltage and Current of SVPWM based full bridge inverter.	33
3.15	THD of SVPWM based full bridge inverter at Full Load.	34
4.1	Clarke and Park transform in three phase system.	39
4.2	General structure of three-phase synchronous rotating reference frame control strategy.	41
5.1	Single Phase Inverter Model with LCL filter.	47
5.2	Single Phase Inverter Scheme.	50
5.3	Single-phase inverter representation as real and imaginary parts of the circuit.	51
5.4	Stationary reference frames model of single-phase inverter.	53
5.5	Controller structure with inner current loop and outer voltage loop.	55
5.6	Feed-forward controller.	56
5.7	Grid tied inverter circuit diagram.	57
5.8	Grid tied inverter detailed circuit diagram.	58
5.9	Full bridge inverter connected with grid and variable load.	58
5.10	Step increase of load.	59
5.11	Alpha-Beta to DQ0 conversion.	59
5.12	Current controller in DQ reference frame.	60
5.13	Current waveforms on increased load demand.	61
5.14	Coupling point Voltage and inverter Current.	61
6.1	Network line power flow.	70
6.2	Line power flow phasor diagram.	70
6.3	Droop curves for active and reactive power.	72
6.4	The inverter set to supply Active and Reactive Power ($S=P+Q$).	74
6.5	Constant power from inverter.	75
6.6	Variable power from inverter to constant load.	75

List of Tables

3.1 Switching status.	27
-------------------------------	----

List of Abbreviations and Symbols

Abbreviations

DER	Distributed Energy Resources
THD	Total Harmonic Distortion
SVPWM	Space Vector Pulse Width Modulation
RES	Renewable Energy Sources

Introduction

1.1 Motivation

Demand in energy is increasing gradually, to overcome the demand and supply gap a lot of alternative solution are under researcher's consideration around the globe. The major sources of energy are fossil fuel in form of crude oil, nuclear energy that uses nuclear reactors, and renewable energy resources. Fossil fuels are the most often used source of power generation till date, but the drawback is the release of harmful gases in the burning process of fuel in order to generate electricity [1]. The harmful gasses are main contributor in the in problem of global warming. To save the environment from the hazard use of renewable energy resources increased to share the energy requirements. Renewable energy resources including biofuels, wind, biomass, solar, hydropower, and geothermal started to be deployed and investigated. Since renewable energy resources being the better substitute of traditional energy sources the increasing trends the usage of signify the need of research in the domain.

Convenient installation of solar powers systems has influenced general public to use such systems. The installation of such systems not only benefits the consumer itself but also to energy system as it reduces the demand form the main grid. Locally installed power systems can supply the surplus power to the grid and alongside consumers. A local power system using solar panels or a wind turbine provides having high reliability and low running cost are a great solution to power needs.

For grid-tied inverter systems performance limits allowable for grid-tied applications must be defined. The most important points are [2]

- Quality of the power injected into the grid.
- Inverter output should be fully synchronized with the utility grid.
- Anti-islanding protection.

Each of these points poses significant challenges in development. Therefore, the inverter systems and the controller task have become more and more complex while optimum solutions are sought. It is evident that simulation and simulation models can support systems development in several ways. Furthermore, simulation offers a safety factor in evaluating techniques as well as reducing the necessary development-cycle time.

It is worth stating that three-phase inverters that provide high performance are often implemented using synchronous rotating reference frame (d-q) controllers. In many cases, developments in single-phase systems have followed the developments in three-phase systems. Therefore, this thesis proposes a method that harnesses the benefits of synchronous rotating frame control but that can also be employed effectively with the single-phase inverter.

1.2 Problem Statement and Proposed Solution on the Inverter Side

Along with the environmental problems discussed earlier conventional power systems include other problems like dependency on one source, Long distance transmission, Power outages, Load shedding, Maintenance (due to aging and faults in lines). This gave rise to the inevitable penetration of Distributed Energy Resources (DERs), wastage of surplus energy, compromise on critical operational load due to low power backup. Solution is to come up with a system changing flow of energy from one way to multi-directions in form of decentralized energy transmission, introduce energy sharing among communities. DC-AC inverters are the core of majority of distributed energy systems. Unlike the conventional energy sources, power sharing and current control in inverters particularly in single phase are not straightforward. However, literature has suggested a few approaches (see Chapter 2). Therefore, the research in this thesis will concentrate on the following points:

1. Developing an efficient converter with low value of Total Harmonic Distortion (THD). A new single-phase inverter switching gate-drive algorithm will be developed, which will improve efficiency while maintaining low THD.
2. Satisfying the international standards [3] on power quality by the developed controller stage.
3. According to the selected method for current control, a control for its operation in grid connected mode will be developed. The role of the controller will be to inject active power and reactive power (where appropriate) with high power quality into the load or the grid. A stand-alone control will also be considered to meet the demand of locally connected load.
4. As the final part of the study, a small-scale individual (decentralized distributed) generator will be developed, with the design of controller so as not to require extensive communications between itself and the electricity supply network.

The objective of this is to build a system working in different modes of operation, by means of:

1. Investigating single-phase inverter gate-drive algorithms based on SVPWM (hitherto commonly used with three-phase inverters).
2. Introducing a new control method for a single-phase inverter by utilizing rotating-frame analysis and control design (until recently only used for three-phase converters), i.e. the well-known vector controller or rotating reference frame controller [4]. This research focuses on introducing an additional control method for single-phase full-bridge inverters to give superior dynamic response and system performance.
3. Investigating the effects of incorporating such systems into the utility network as decentralized distributed generators.

Decentralized distributed generators allow generation of smaller amounts of power in a lot of places, rather than a lot of power in one place. This leads to electrical power being generated nearer to the point at which it is consumed. Consequently, this allows more power to travel with lower losses to customers in cities, towns, as well as rural areas. This can make optimal use of small-scale energy generation, as well as allowing the use

of the renewable energy sources. Such converters can operate in autonomous mode, can be connected together, or can be used in grid-tied mode.

The single-phase inverter circuit analysis and controller design is described in this thesis. The proposed controller is developed and verified with the use of MATLAB/SIMULINK.

1.3 Thesis structure

The organisation of thesis is arranged as follows

Chapter No.2 Literature Review and Design Considerations: This chapter discusses some part of literature review including the inverter, filter and previously used current control strategies. Considering the literature design scheme of LCL filter is discussed.

Chapter No.3 Space Vector Pulse Width Modulation: In this chapter SVPWM approach of Single Phase inverter is discussed.

Chapter No.4 Theoretical Aspects of Stationary and Synchronous Rotating Frame: this chapter shows the theory of two types of reference frames and their contribution in grid tied inverter control.

Chapter No.5 Single Phase Inverter Modeling Based on Synchronous Rotating Frame: Derivation of mathematical model in synchronous rotating frame is performed in this chapter. Single phase inverter is assumed to be connected with grid and load. Model is tested with different types of load.

Chapter No.6 Droop Control in Synchronous Solid-State Converter: In this chapter the droop control method of inverter is discussed with simulation of active power and reactive power being transferred to the grid and load.

Chapter No. 7 Conclusion and Future Work: The summary of work that is presented in this thesis and future work is discussed.

Literature Review and Design Considerations

2.1 Introduction

This chapter includes the literature overview of the proposed research area. The beginning of this section describes the international standards required in the design of a small-scale renewable electrical system. Then, the inverter unit and its operations is discussed. Inverter control methods are reviewed, and a new control approach is suggested for small-scale inverter systems in the grid-tied mode under a decentralized power supply strategy. Consequently, the design considerations such as inverter output filter design calculations are also considered in this chapter.

2.2 Standard Permits for Grid Connected Inverter System

Standards and regulations specifically for power system exist, such as the IEEE Std. 519TM-2014 [3]. It contains relevant requirements for small-scale inverter systems of 69kV or less. According to these standards the THD that is calculated at the the output voltage should be lesser than 5%.

There are other standards in the world, some with fewer and some more stringent restrictions. The work in this study focuses on meeting the most stringent standards and their requirements. National electric power regulatory authority provides standards for nominal voltage and frequency in Pakistan following IEEE Standard 519.

2.3 Voltage Source Inverter: Structure and Operation

Considering the inverter unit as the core unit in the systems for the AC power interfacing purposes. This study will focus on single-phase inverter development particularly in the inverter gate-drive and the controller side. Therefore, it is worthwhile looking at the components and the functioning of the inverter before starting the development process.

2.3.1 Single Phase Inverter

In single-phase applications, the full-bridge and half-bridge inverters represent the basic circuit topologies, while multilevel inverters and Z-inverters represent a further development approach retaining the fundamental inverter circuit methodology. Different circuit design approaches are used to focus various issues. The design approach also depend upon the intended use of inverter.

The basic circuit of a single-phase full-bridge inverter, which is used for converting a DC voltage to an AC voltage, is shown in figure 2.1. This type of inverter operates from a positive and a negative DC source and produces AC voltage.

The switching transistor S1, S2 is driven complementary to switching transistor S3, S4. The transistor S1, S2 conducts during the first sub-interval $0 < t < \delta T_{sw}$ (where T_{sw} is inverter switching period), while S3, S4 conducts during the complementary sub-interval $\delta T_{sw} < t < T_{sw}$. The volt-second balance across the inductor is given in Eq. 2.3.1

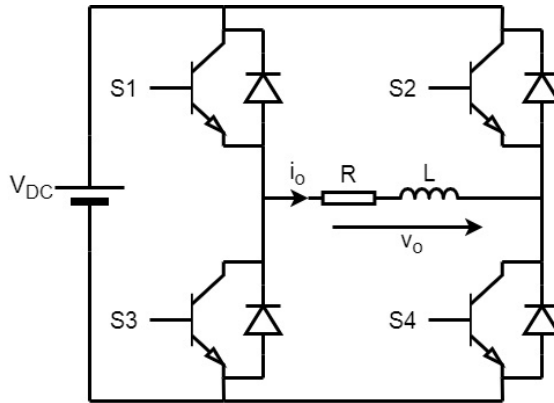


Figure 2.1: Single Phase Full Bridge Inverter.

$$V_O = \delta V_{DC} - (1 - \delta)V_{DC} \quad (2.3.1)$$

$$V_O = (2\delta - 1)V_{DC} \quad (2.3.2)$$

Where δ is duty cycle ($1 \geq \delta \geq 0$) and $T_{SW} = t_{ON} + t_{OFF}$. The relationships between switching on/off time t_{ON}, t_{OFF} intervals and the switching period T_{sw} are given by,

$$\begin{aligned} t_{ON}/T_{sw} &= \delta \\ t_{OFF}/T_{sw} &= 1 - \delta \end{aligned}$$

With an output filter inductor, the inductor current positive slope occurs during δT , and its negative slope during $(1 - \delta)T$. The load current (V_O/R) coincides with the inductor current (i_L) in the equilibrium state.

$$L \frac{di_L}{dt} = V_O - V_{DC}(2\delta - 1) \quad (2.3.3)$$

Since the load usually contains inductive components, the load current will lag the fundamental voltage. Anti-parallel diodes are connected for the peak inductive load current to flow through them when the switch is turned off state. Notice that parallel transistor switches on the same leg cannot be in the on-state at that moment, else it will short circuit the DC supply and consequently destroy the switching devices.

The Voltage are generated in a fashion that switching circuit receives gating signals from the Pulse Width Modulator and the power electronic semiconductor switches are switched on and off. This leads to an output voltage that has a desired fundamental component, but also contains switching harmonics. These undesirable harmonics are filtered out through a passive filter and the current transferred into the grid is a nearly perfect sinusoid.

If the output current is measured or sensed and then it is compared with a reference, we get an error signal. This is fed to an appropriately designed controller which produces a control signal. This is transmitted to the Pulse Width Modulator which generates the desired gating signals. If properly implemented the closed loop operation results in steady state error to be zero steady state error and the output current tracks the reference given to the control system.

2.3.2 Modulation Strategy

In some cases, the development of the inverter involves changes to the switching gate-drive algorithm e.g. pulse-width modulation (PWM), sinusoidal pulse-width modulation (SPWM), and space-vector pulse-width modulation (SVPWM) in addition to developments of the inverter controller.

The quality of the output voltage of inverter depends on the number of harmonics and the magnitude of each harmonic that exists in the output voltage. The inverter output quality can be measured by many parameters; the most important ones are the magnitude of individual (nth) harmonics (HF_n), and the total harmonic distortion (THD). Various modulation techniques such as PWM, SPWM and SVPWM are proposed in the literature to increase the quality of inverter output. These techniques are now commonly used for controlling inverter output voltage and current. Some of these techniques are further modified so as to increase the inverter performance and reduce the THD. All these techniques share the same principle of operation, i.e. switching the supply on and off and power up the load at a high pace (to perform PWM), the frequency of which is referred to as the carrier frequency. Another important term that is linked with PWM and the most important factor is the duty cycle (δ) that shows the relation between the duration for how long the switch is turned on (t_{ON}) with respect to the total switch period (T_{SW}) in form of percentage ratio.

2.3.3 Filters

The output of the inverter is in form of switched voltage pulses that are at a constant switching frequency and contain a wide range of harmonics. Inductors and Capacitors are used to attenuate the high frequency harmonics and switching noise, they can be combined in different ways to construct passive filters. Generally, low-pass passive filters should be designed to allow the fundamental waveform component to be passed while reducing the contribution of harmonic components in output. Commonly used passive filters for power applications are

1. L Filter
2. LC Filter

3. LCL Filter

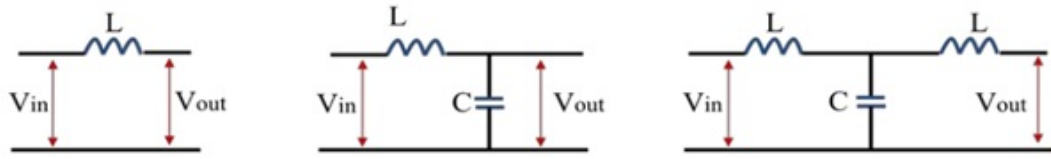


Figure 2.2: Filter Configuration Circuits.

1 - L Filter: This represents a first order filter giving -20 dB/decade roll-off into the stop-band. This type of filter achieves only a low level of attenuation of the inverter switching frequency components. Therefore, if one wants to achieve satisfactory attenuation of the output harmonics, the inverter switching frequency has to be much higher than the fundamental frequency [5].

2 - LC Filter: This represents a second order filter that are used to get -40 dB/decade attenuation in the output. In this type of filter, capacitor is connected in the shunt to facilitate attenuation in the switching frequency, but the value of capacitor must be chosen carefully so that it maintains low reactance at switching frequency while posing higher impedance within the control frequency range. In the cases where the system uses an isolating transformer at the low-frequency side, the LC filter can fulfil the harmonic limit requirements [6].

3 - LCL Filter: This type of filter is a third order filter that gives good attenuation of -60 dB/decade. This type of filter can reduce the harmonic distortion levels at lower switching frequencies. LCL-filters are also suitable where Even the low values of L and C can demonstrate exceptional attenuation ratio. Nonetheless, one must be careful while designing the third order LCL filter and consider several design constraints, such as the current ripple that is flowing through inductors, the resonance frequency, the output impedance of the filter, the attenuation of the harmonics induced in current due to the switching frequency, and the amount of reactive power that the capacitor absorbs etc. [7].

2.4 Methods for Inverter Current Control

Applications where sinusoidal AC output is desired from an AC-DC inverter with the control of output magnitude and frequency, control of current becomes an important factor, particularly in grid connected modes. Tracking of the reference current and providing corresponding output is the main activity of current control, with acceptable transient performance without poor dynamic response, undesirable overshoot or undershoot.

Total harmonic distortion should be less than the threshold values defined as the standard. Competitive cost and size of the converter are the deliverable objectives of the current control. Following section discusses the methods for current control of single-phase inverters.

2.4.1 Linear Regulator Based Method

The current at the output of inverter is controlled with carrier-based PWM (the so-called carrier-based method). This method has been modified in several studies to decrease the THD that is induced in the output current of inverter. The methods used, in which the PWM is modified to revamp the quality of the current waveform are: the SPWM methods, centroid based switching, hybrid PWM and random hybrid PWM. Figure 2.3 represents a simplified diagram to describe the carrier-based control method. Proportional Integral control (PI) has poor performance when tracking a sinusoidal reference due to the steady-state error at frequencies other than DC. Moreover, this controller is not capable of reducing noise in the current signal. The system tends to be slower to reach the set point and slower to respond to perturbations. As a result, it can generate an overshoot in the present value while trying to achieve the set point value. In the case of linear regulators, the main advantage of the control method based on carrier is its constant switching frequency.

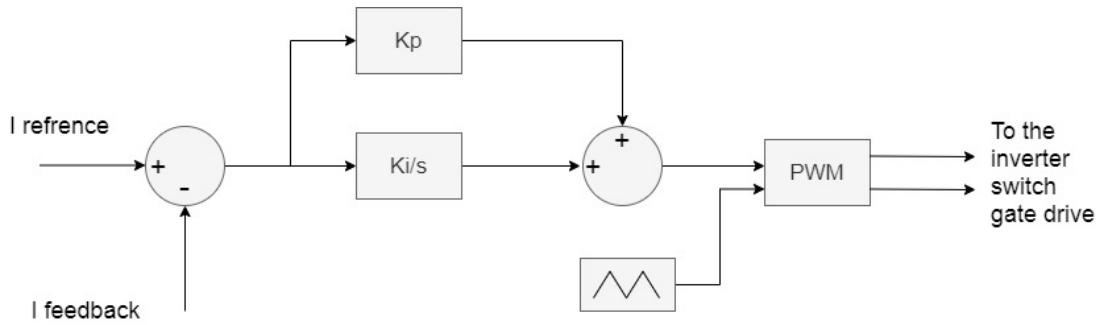


Figure 2.3: Carrier-based current control method.

[8] Proposed another modification to the carrier-based method. This is by combining the PI current control transfer function with a sinusoidal transfer function, as shown in figure 2.4. The resonant frequency brought about by the additional term is equal to the utility frequency. Consequently, the current controller which is proposed can fulfil the provision of infinite gain at the line fundamental frequency.

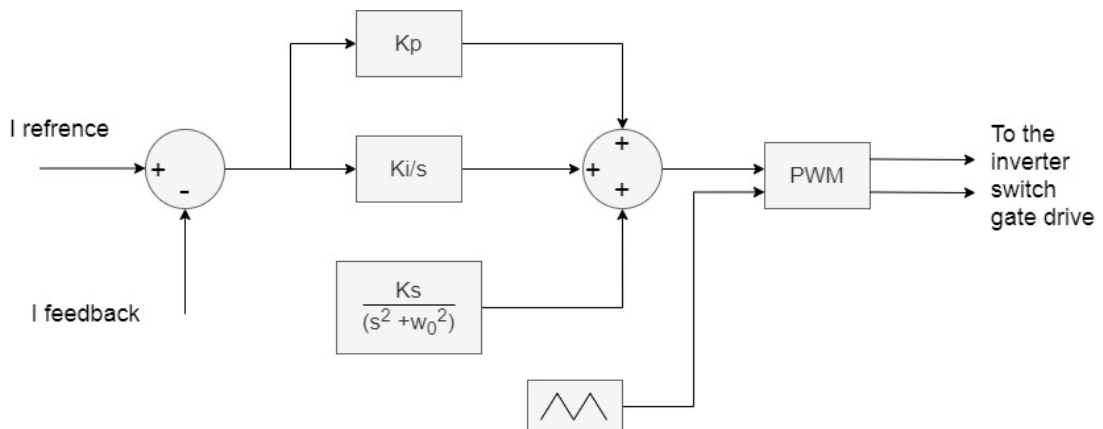


Figure 2.4: Carrier-based controls scheme with sine transfer function.

The disadvantages are that the compensator has a slow response, and it is very sensitive to variations in the fundamental frequency, as well as having a high phase margin around the line frequency [9], which can cause instability in the system. The general drawback of the carrier-based method as compared to other direct current control methods is the poor dynamic response of linear compensators, which causes poor overall transient response.

2.4.2 Hysteresis Control Method

The hysteresis current control method is implemented by dedicated hardware and can have acceptable transient performance. In this method, the current reference is followed by the inverter output current. The upper and lower band in a hysteresis loop limits deviation between reference and output current, see figure 2.5. This also guarantees a peak current limiting capability.

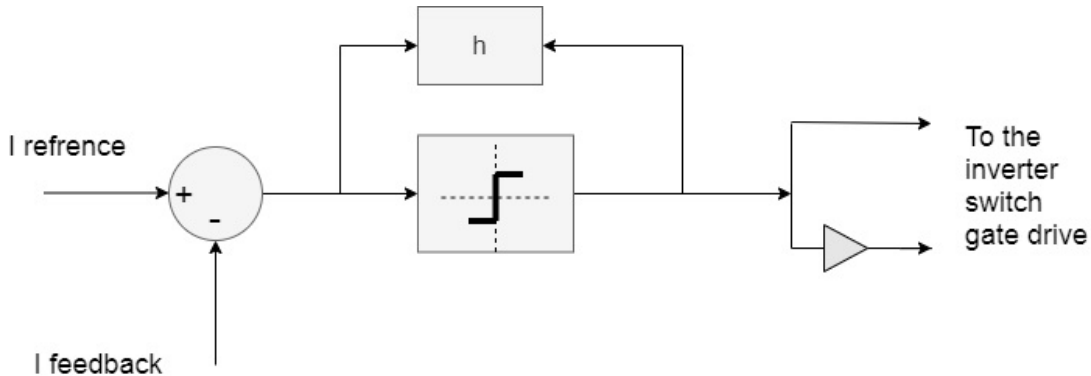


Figure 2.5: Hysteresis current controller scheme.

At all the points of switching frequency, peak to peak ripple current is needed to be controlled causes the change in PWM switching frequency, this is the disadvantage of this technique. Due to the change in PWM switching frequency varies, this causes to produce high THD. To overcome this variable switching frequency problem of the hysteresis method, some modified hysteresis methods have been proposed, such as a three-level hysteresis current control strategy [10], another approach that define both the bands of hysteresis controller (i.e. upper and lower band) is introduced by the name of 'random hysteresis method' [11]. These methods deliver an output current with narrow frequency spectrum content. Variations in system parameters may affect the performance of the controller. Generally, with hysteresis controllers, there will be a wide bandwidth of harmonics in the inverter output current.

2.4.3 Proportional-Resonant Current Controller

PI controllers are very common in DC-to-DC converters, but the performance is not so good in inverter applications. This is because a sine wave signal is required to be tracked, which is devious in comparison to the tracking of a DC signal. While tracking

sinusoid reference signal, time invariant steady state error is produced. Furthermore, low rejection of noise from the current signal is evident. [12] Introduced the Proportional-Resonant (PR) current controller. In this approach an AC compensator is introduced in contrast of classical PI DC-compensator that has the similar frequency response characteristic in the concerned bandwidth. There are several advantage is using PR controllers, authority over the controlling individual resonating peak in the grid frequency and provision of precise tracking, to some low-order harmonic frequencies for selective harmonic compensation. another possibility is to create a reference generator for harmonics for active filter of harmonics. To the variation in fundamental frequency their response is highly sensitive. The response speed is low, large phase margin can cause very high stability problem around the main frequency. These disadvantages makes it a less suitable choice.

2.4.4 Synchronous Rotating Frame Controller

The scheme design of compensation in current-error is critically important especially within grid-tied single-phase inverter applications. Among the previous developments of current controllers and making use of the experience with the three-phase inverter are [13], which employs current control strategies based on a separate current controller (current error compensation) and a PWM function that can exploit more advantages in an independently designed overall controller structure [14]. Since the synchronous rotating frame controller was proposed for this study, Chapters 4 and 5 will give more details about this type of controller.

2.5 Decentralized Power Supply

Most power plants are built in a large scale due to a number of factors that include economics, safety, logistic, environment and some of the geographical and geological factors. This is because the major contribution in the energy from the large scale centralized power plants is from the ones that use fossil fuel, nuclear power or hydropower. There are number of drawbacks with such centralized systems, including:

- The high level of dependence on non-renewable fuels.
- Environmental impact.

- Losses occur in the transmission and distribution.
- Higher cost of generation plants, transmission and distribution network.

It is known that the rate of growth of electricity demand is on the rise [14]. In addition, requirement of the energy for services is estimated to increase considerably due to the increasing level of services in modern economies. A system that include various type of sources that produce energy is considered to be more secure and redundant. This study encourages the idea of incorporating a small-scale renewable energy power supply into domestic dwellings as part of the power network. With this idea, a huge quantity of small-scale decentralized power supplies would be connected to the power network, which may increase the complexity of the power supply control systems. The work in this study simplifies the inverter-grid load sharing. The inverter side controller uses grid parameters which can be measured at the inverter-grid common coupling point without extensive communications. This is achieved by using the droop function method, this method is considered to be efficient in usage of small scale renewable energy sources [15–17]. In this method, the references for active and the reactive power determines the reference for current, that result voltage and frequency droop control - controlling the inverter output power by manipulating the voltage magnitude and shifting in the phase (the changing of angle between the inverter output voltage and the grid voltages) depending on locally-measured instantaneous information. The synchronous rotating reference frame controller can be provided with the inverter active and reactive output power control to support the suggested droop strategy. In this method, modulation index controls the reactive power, whereas the phase shifting controls the active power. Chapter 6 gives more details about this strategy.

2.6 LCL Filter Design Consideration

LCL filter is a third order filter, it can provide high attenuation of switching frequencies even with the low values of capacitor and inductors. [18] Describes the procedure of designing a LCL filter, various parameters must be kept under consideration during the design such as desired current ripple, attenuation in the switching ripple and resonance in the capacitor that connects with the grid. Both active and passive damping approaches are considered while designing the LCL filter. In this design active damping technique is

used. Figure 2.6 show the algorithm used in design of filter design.

The parameters of the filter should be decided before the filter design that include inverter output RMS voltage, DC-link Voltage, rated active power, switching frequency and resonance frequency. The step by step details of designing the filter is discussed as follow.

The base values will be calculated first and then the filter values will be referred to in their percentage. to calculate the base impedance and base capacitance nominal voltage, power and grid frequency is required,

$$Z_b = \frac{E_n^2}{P_n} \quad (2.6.1)$$

$$C_b = \frac{1}{w_g \cdot Z_b} \quad (2.6.2)$$

Where, E_n is the nominal input voltage, P_n is the nominal power that is decided for the inverter and w_g is the nominal frequency.

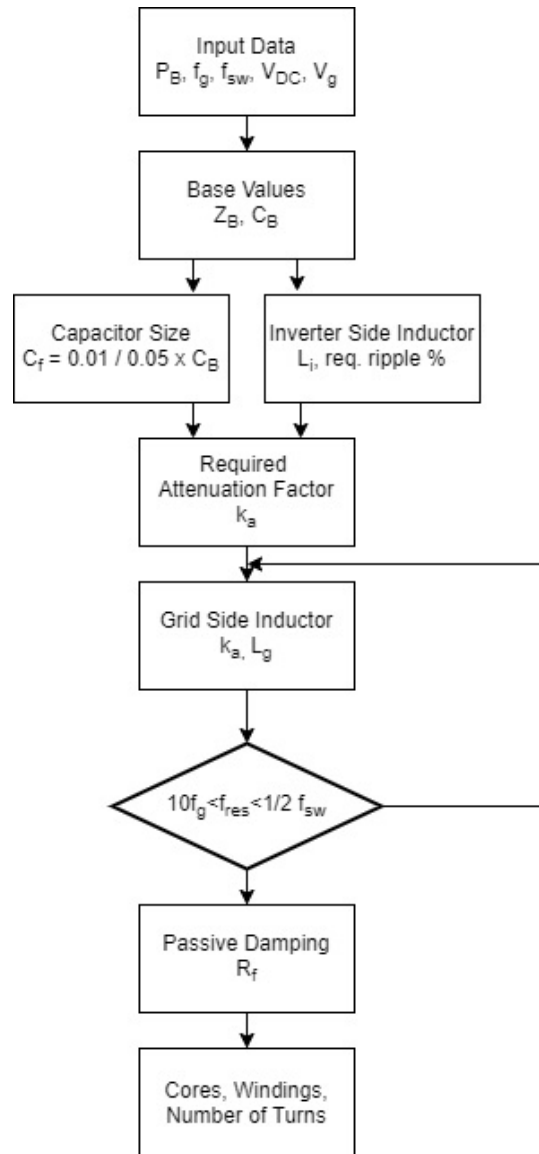


Figure 2.6: LCL filter design algorithm.

The maximum variation in the power factor is considered to be 5%, this is important while calculating the value of filter capacitor, this indicates the adjustment of base impedance as under

$$C_f = 0.05C_b \quad (2.6.3)$$

If compensation in the reactive power that is occurring due to the inductor used in filter is desired, a higher value of design factor that 5% can be used. The maximum value of ripple current (ΔI_{Lmax}) produced at the output of inverter can be calculated as,

$$\Delta I_{Lmax} = \left(\frac{2V_{DC}}{3L_i}\right)(1-m)(mT_{SW}) \quad (2.6.4)$$

In the above equation m is the modulation index (typically in SPWM inverter). from the above equation it can be deduced that at the value of $m = 0.5$ maximum value of peak to peak current ripple are produced, considering this condition the equation can be rewritten as,

$$\Delta I_{Lmax} = \frac{V_{DC}}{6f_{sw}L_i} \quad (2.6.5)$$

Where, L_i is the inductor located at inverter side of filter. The rated output current for the design with the ripple value of 10% can be given as,

$$\Delta I_{Lmax} = \frac{0.1}{I_{max}} \quad (2.6.6)$$

Where, I_{max} is the maximum current of inverter. The inverter side inductor is calculated by,

$$L_i = \frac{V_{DC}}{6f_{sw} \cdot \Delta I_{Lmax}} \quad (2.6.7)$$

The current at the output of filter is desired with the reduction of ripple to 2%. This result the ripple value at the output current is of 2%. Equations 2.6.8 and 2.6.9 shows the relation between the current transferred to the grid with the harmonic current that is created by the inverter.

$$\frac{i_g(h)}{i_i(h)} = \frac{1}{|1 + r [1 - L_i C_b \omega_{sw}^2 x]|} \quad (2.6.8)$$

$$L_g = \frac{\sqrt{\frac{1}{k_{sw}^2} + 1}}{C_f \omega_{sw}^2} \quad (2.6.9)$$

Where, ka represents the desired attenuation, $x = 0.05$ - according to the design maximum power factor variation at the grid $C_f = 0.01/0.05C_b$, and the ratio of both the inductors i.e. at the grid side and at the inverter side is given with the constant r is .

$$L_g = rL_i \quad (2.6.10)$$

Depending on the nominal grid impedance, results can be plotted for various values of R . For a particular resonant frequency these plots will be helpful in figuring out the transfer function. Resistor (R_f) is connected with the capacitor in series to attenuate the ripples in the output, hence reducing the harmonics. First the impedance of capacitor is calculated at the resonant frequency, then the value of resistor (R_f) is calculated as the one third of the impedance value of capacitor. The formula for calculating the value is given in 2.6.11.

$$R_f = \frac{1}{3w_{res}C_f} \quad (2.6.11)$$

Where, w_{res} is the resonant frequency and its range is satisfied by Eq. 2.6.12 and 2.6.13

$$w_{res} = \sqrt{\frac{L_i + L_g}{L_i L_g C_f}} \quad (2.6.12)$$

$$10f_g < f_{res} < 0.5f_{SW} \quad (2.6.13)$$

10,000 Hz switching frequency was selected for 4.5kW, 230V inverter. As a result, L_i and L_g were calculated as $2.93mH$ and $0.92mH$ respectively and C_f and R_f were calculated as $16.5\mu F$ and 0.78Ω respectively. Bode Plot of the designed LCL filter presented in figure 2.7

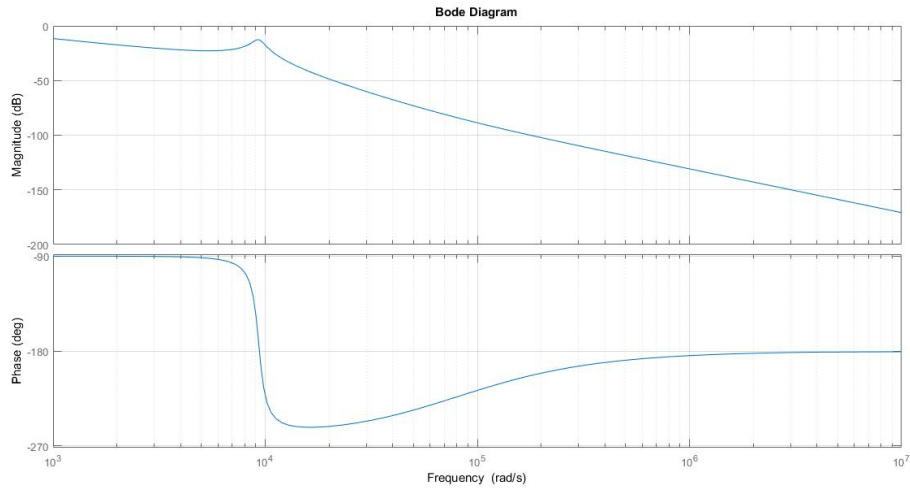


Figure 2.7: LCL filter bode plot.

Space Vector Pulse Width Modulation

3.1 Introduction

Modulation techniques that are used to generate gate drive signals are discussed in this chapter. The purpose of modulation is to minimize the switching losses and harmonics while obtaining a variable output. Inverter output can be fairly improved by moving the harmonic component to higher frequencies.[19, 20] To enhance the inverter output spectrum, correct choice of PWM scheme should be used. In three phase inverters Space Vector PWM (SVPWM) approach is considered to be a favorable choice among the other PWM approaches. It enhances the utilization of inverter hardware, this approach intrinsically limits the effect of an inherent third harmonic injection [21] and simplifies the control organization.

Each PWM technique has its own benefits. Almost all of the techniques are tested on both single phase as well as the three phase inverters. SVPWM in particular has been applied over three phase inverters and proven to be quite worthy. This technique has not been extensively tested on single phase inverters. In this chapter, SVPWM approach is designed for execution on single phase inverters. MATLAB (Simulink) environment was used for testing and simulation of design. Outcome showed commendable response in terms of reduction in THD and provided high modulation index in comparison to the conventional Sinusoidal PWM (SPWM) technique.

3.2 General Description of Pulse Width Modulation Techniques

Several techniques based on pulse width modulation (PWM) strategies are commonly used today as part of the control of solid-state power supplies. Switching frequency, duty cycles and properties of the load are the contributor to the ripples in voltage in current. To get better results from traditional PWM techniques compromise are made in form of high switching frequency and increasing the size of passive filter.

Power can be easily controlled with the help of PWM in semiconductor switched. They provide low power loss, but it's observed that there during the switching cycles over the fundamental frequency voltage and current become non-zero. This causes high power dissipation on the switched. However the power loss is still low in comparison to the delivered output power even when high switching frequencies are used.

During the switching period the power drop over the semiconductor switches is quite low either switch is in the on state or in the off state. However, when the switches are in the transition from on to off or off to on state, considerable amount of power is dissipated since the voltage and current both are non zero. Insulated gate bipolar transistors (IGBT) and MOSFET are suitable switching for power circuit implementations as they provide high efficiency and fast response.

Pulse width modulation produces a rectangular periodic pulse train whose duty cycle varies depending on the average value required at the output side, as shown in figure [3.1](#)

The objective of PWM is that for a given switching period, obtain an output signal which is equivalent to the provided reference signal. Following the pattern provide a train of pulses in which the fundamental component of the frequency is reflected, and meet the requirement of volt second average of the target wave at any instant of time. Several techniques are applied using different arrangement of switching schemes in order to minimize the distortion, unwanted harmonics and switching losses.

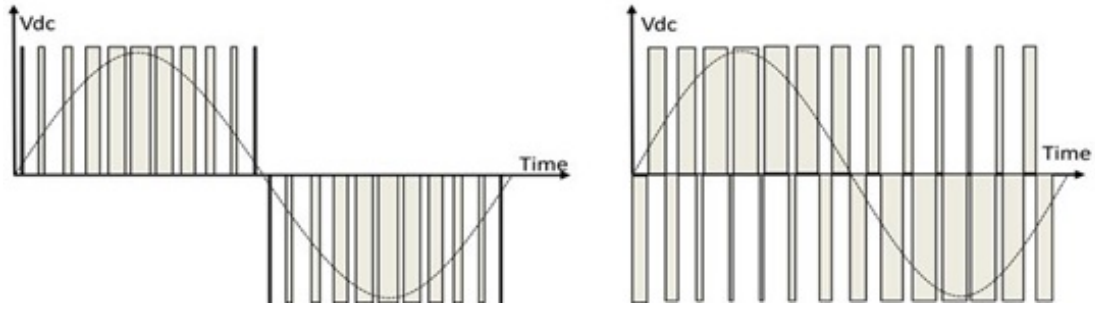


Figure 3.1: Unipolar PWM and Bipolar PWM.

3.3 General PWM Classification

Several modulation strategies have been developed. There are many possible PWM techniques proposed in the literature; these differing in concept and/or performance. The important techniques are:

- Hysteresis-band current control PWM.
- Synchronized carrier modulation.
- Sinusoidal PWM (SPWM).
- Space vector PWM (SVPWM).

Hysteresis-band PWM and synchronous carrier modulation techniques employ variable switching frequency strategies in which carrier frequency varies with the output waveform. SPWM and SVPWM are fixed (constant) carrier frequency strategies. The fixed frequency strategies share some common features:

- Switched pulse width determination.
- Switched pulse position within the carrier interval.
- Switched pulse sequence across and within the carrier interval.

3.4 Hysteresis Current Controllers

The basis of hysteresis current control is quite straightforward. A reference signal is forced to be followed by the controller. The current is kept within the hysteresis band

by regulating the switching action of inverter. Figure 3.2 shows the principle.

The lower limit of the hysteresis band indicates to low value of output current, whereas, the upper limit indicates the high value of output current. The output voltage waveform is analogous to the bipolar PWM output voltage.

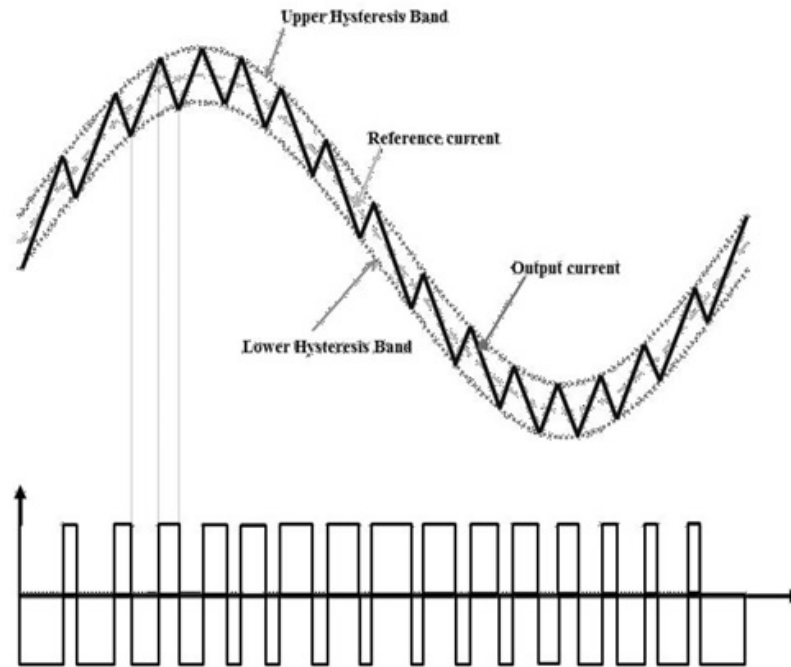


Figure 3.2: Hysteresis current controller PWM.

Hysteresis current controllers have the advantages of simplicity, provision of instantaneous current corrective response (subject to slew rate limitations), and unconditional stability of the system. The drawbacks of this method are that the switching frequency is variable and largely depends on the load parameters that may vary widely. Consequently, the load current harmonic ripple is not optimal. This leads to a wide range of variable switching frequency, causing a wider noise bandwidth.

3.5 Sinusoidal PWM

In this approach, a sinusoidal reference signal (i.e. the modulating signal) is compared with a triangular carrier-wave signal to generate gate pulse signals at the points of intersection between the carrier signal and the modulating signal. Figure 3.3 shows the principle of switching gate signal generation with SPWM.

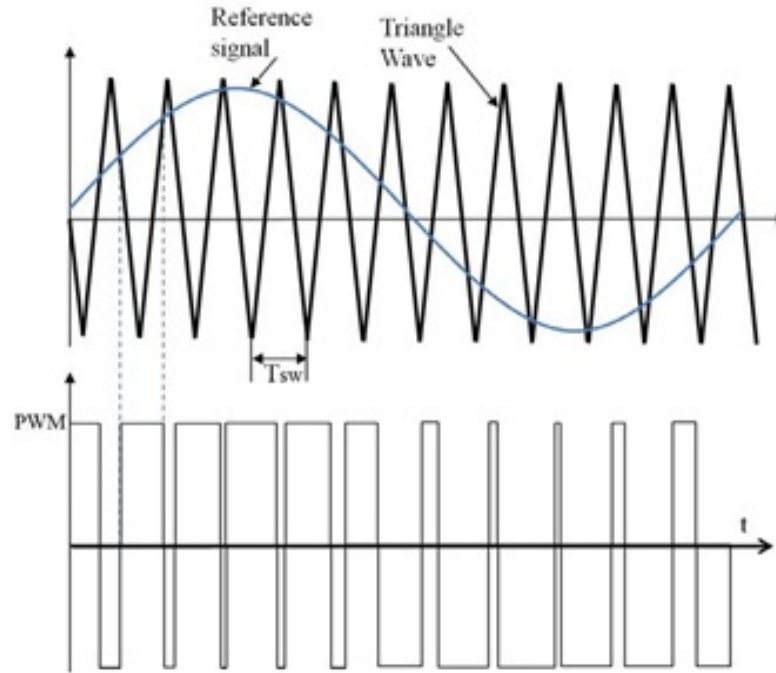


Figure 3.3: Sinusoidal PWM generation.

The modulation index (m) is defined as:

$$m = \frac{V_p}{V_t} \quad (3.5.1)$$

Where V_p is the peak of the modulating wave and V_t is the peak of the carrier wave. Ideally, the relation between the output wave magnitude and the modulating wave is linearly regulated by setting the value of modulation index between 0 and 1. The inverter fundamentally behaves as a linear amplifier with a specific gain between the modulating/reference signal and the output voltage.

The magnitude of the higher harmonics is independent of the carrier frequency. At higher carrier frequencies, the inverter output harmonics will be significantly attenuated by the output filter, and the output voltage and current waveforms become closer to a sinusoid. The selection of carrier frequency depends on the trade-off between the inverter loss and the output waveform quality. Higher carrier frequencies increase inverter switching loss but decrease the output filter cost and size while reducing the output waveform distortion.

3.6 SVPWM Technique

In recent years, the use of SVPWM has overwhelmed SPWM in three-phase inverter control systems. The former provides for a more competent use of supply voltage in comparison with other modulation techniques. It appears to be the best technique for three-phase switching power inverters and has become commonplace in three-phase voltage-source inverters. SVPWM can increase the available DC voltage link utilization ratio (modulation index) significantly. SVPWM techniques have been the under the light of intensive research for various different industrial applications in three-phase voltage-source inverters, [22] The advantages of 3-phase SVPWM are summarized below:

- Its output voltage is higher than regular SPWM for a given DC-link voltage
- Total harmonic distortion (THD) is minimized
- Excellent exploitation of DC supply voltage is achieved.
- The arrangement of vectors provide liberty to reduce the switching loss. Or even to obtain a different kind of result, such as center-aligned PWM, edge-aligned PWM, minimal switching [23].
- Gives a high control over the variation of space vectors during the PWM, could be zero or non-zero.
- It is easily implemented digitally.

3.7 Space Vector Concept

The space vector fundamentally arise from the rotating field theory of three-phase induction motors. It refers to a special switching scheme based on the representation of three-phase voltage quantities as two equivalent orthogonal variables in the phasor diagram. These two equivalent orthogonal components can then be represented either in a stationary reference frame or a synchronously rotating frame (rotating at angular speed w) by using the Clarke and/or Park transformation. The SVPWM technique was developed as a vector approach to three-phase pulse width modulation [23].

SVPWM is a digital modulation technique typically implemented in software using a microcontroller or digital signal processor [23]. The goal of SVPWM is to generate

The appropriate PWM signals so that the vector quantities (such as voltages or currents) can be represented by time weighting and averaging. This is done by approximating the reference quantity (voltages or currents) instantaneously using a weighted arrangement of the switching states corresponding to the basic space vectors in the time domain. For a short period of sample time, the average inverter output voltage is the measured to have the same value same as the average reference voltage during the sample time, i.e. the length of the vector and amplitude of the fundamental voltage is directly proportional.

3.8 The Basic Principle of SVPWM

Three-phase SVPWM is implemented by using a transformation from three-phase time-variant quantities to two orthogonal time-invariant quantities. This can be represented as a voltage vector projected onto a two-dimensional vector plane. The elementary idea of space vector modulation is to develop the required volt-second product across the output inductor using discrete switching states. The SVPWM can be implemented by the following steps:

1. Define the possible switching vectors. For a simplified representation, it is possible to include a coordinate transformation in the output voltage space. The gate signals for the inverter are generated by simple mapping scheme.
2. Define the sector planes and determine the location of desired sector for the voltage vector used in the algorithm, where every sector plane is bounded by two or more vectors.
3. Define the boundary planes. Determine whether the given voltage vector can be implemented with the inverter topology.
4. Switching sates are defined in form of switching sequences. These are actually the states that are applied over a switching period. These switching sequences are stored in the memory. The arrangement of a switching sequence depends on the trajectory of the vector projected onto the mapping unit. This is then used to generate gating signals for the inverter. The switching sequence should minimize switching losses and THD.

5. Determine the time duration. On-time equations are generated by calculating volt second balance these calculations are performed by using geometry mapping. At any switching period with a given algorithm map as well as instantaneous modulation parameters, the processing unit will determine the location of the reference vector and identify the switching state. The switching states can be directly applied to generate signals. This is because switching state represents a exclusive arrangement of "ON" or "OFF" condition for the switches of the inverter

The three-phase SVPWM principle can conveniently provide an initial point for the development of single-phase SVPWM.

3.9 Software Implementation of Single-Phase SVPWM

The single-phase full-bridge inverter contains four switching elements switched in a complementary manner. Since this inverter can generate a single vector, the output voltage vector space can be depicted in a one dimensional space, as shown by the vector at the bottom of figure 3.4.

In order to provide an output voltage equal to the demanded voltage, the switching strategy combines average adjacent vectors during each switching period (T_{SW}). For this purpose, the nearest possible switching vectors are used.

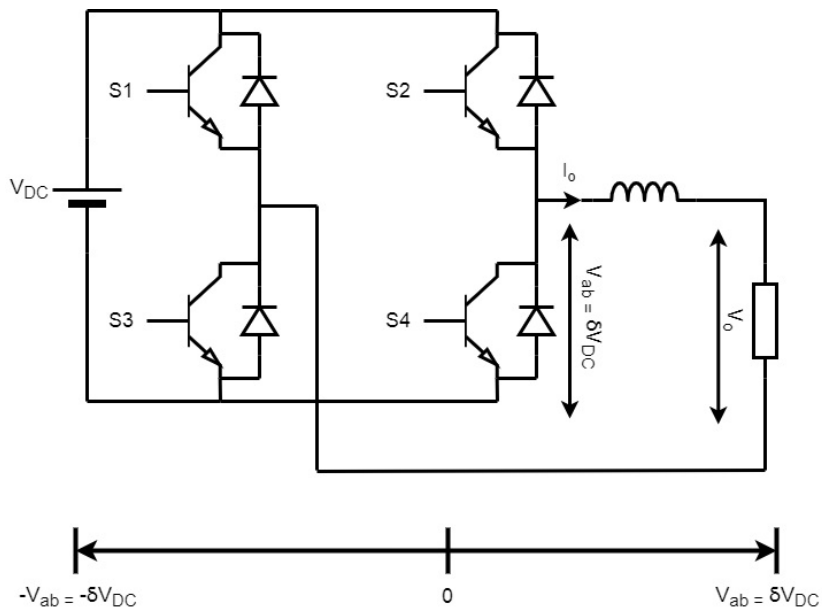


Figure 3.4: Output vector direction of single-phase inverter.

3.9.1 Boundary and Separation Planes

Generally, the output voltage of the single-phase inverter (before the filter) at any instant can be one of three quantities only ($+V_{DC}, 0, -V_{DC}$). Therefore it can be identified by two vectors and indicating two complementary switching signals and a zero state. The possible outcomes are given below:

1. Sector 1, where $V_{ab} > 0$.
2. Sector 2, where $V_{ab} < 0$.
3. Consequently, the separation plane is given by $V_{ab} = 0$.

3.9.2 Switching Sequences

As mentioned previously, the desired switching sequence can be achieved with the nearest adjacent vectors; this will yield smaller output ripples. The operating states of the switched in inverter can be defined by the binary numbers. The vectors V^1 and V^3 shown in Table 3-1 are active vectors, while vectors V^2 and V^4 are zero (or null) vectors. It can be noted that in the V^2 represents the zero vector while vector V^4 is only possible in full bridge inverter.

Table 3.1: Switching status.

<i>Vector</i>	S1 and S4	S2 and S3	V_{ab}
V^1	1	0	$+V_{DC}$
V^2	0	0	0
V^3	0	1	$-V_{DC}$
V^4	1	1	Undesired state

It is necessary to normalize the reference vector length to the base vector. The reference vector magnitude can be limited to V_{DC} by multiplying the reference vector by the coefficient ($1/V_{DC}$) in order to normalize the length of the resultant vector. The reference voltage vector is V_{ref} in SVPWM and it is constructed from the adjacent vectors of the located sector. In order to generate the switching pattern, the reference voltage vector

is transformed into the time-weighted average of adjacent vectors. Therefore, the next step is to compute the duration time of the switching state.

3.9.3 Time Duration

The switching time duration can be computed by applying each switching vector in each switching period T_{SW} . The time duration in the single-phase inverter can be derived through the two following approaches.

3.9.4 Bipolar SVPWM

Bipolar PWM can be achieved when the switching period T_{SW} includes two active vectors in addition to one zero vector. In this case, the vectors can take the following sequence: $V^1 \rightarrow V^2 \rightarrow V^3 \rightarrow$, see figure 3.5.

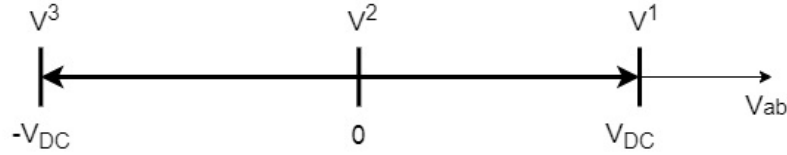


Figure 3.5: Single-phase inverter vector sequence.

The above sequence is described mathematically below:

$$\int_0^{T_{sw}} V_{ref} dt = \int_0^{t_1} V^1 dt + \int_{t_1}^{t_2} V^2 dt + \int_{t_2}^{t_3} V^3 dt \quad (3.9.1)$$

Where t_1 , t_1 , and t_3 are the switching transition instants. As the vectors V^1 and V^3 are active vectors, while V^2 is zero vector, the above equation can be rewritten below:

$$V_{ref} T_{sw} = V^1(t_1 - 0) + V^3(t_3 - t_2) \quad (3.9.2)$$

Where $(t_1 - 0) = \Delta ta$ is the time duration of vector V^1 and $(t_3 - t_2) = \Delta tb$ is the time duration of vector V^3 .

$$V_{ref} = \frac{1}{T_{sw}} [V^1(\Delta ta) + V^3(\Delta tb)] \quad (3.9.3)$$

Where $\Delta ta = Ta$ and $\Delta tb = Tb$, which are the respective time durations for which the switching states corresponding to V^1 and V^3 are applied. However, if we assume that the change in reference voltage V_{ref} is small within T_{sw} , where $Ta + Tb < T_{sw}$, then the residual switching period is reserved for zero vectors. The time duration (T_o) of zero vector is given by.

$$T_o = T_{sw} - (Ta + Tb) \quad (3.9.4)$$

When the voltage at the output of the full-bridge single-phase inverter approaches zero at 0 and $n\pi$ phase-angles of the reference waveform, $Ta = Tb$, and T_o reaches maximum value. Inverter output voltage at its maximum positive value leads to Ta having a maximum weighting, while Tb and T_o have minimum weighting.

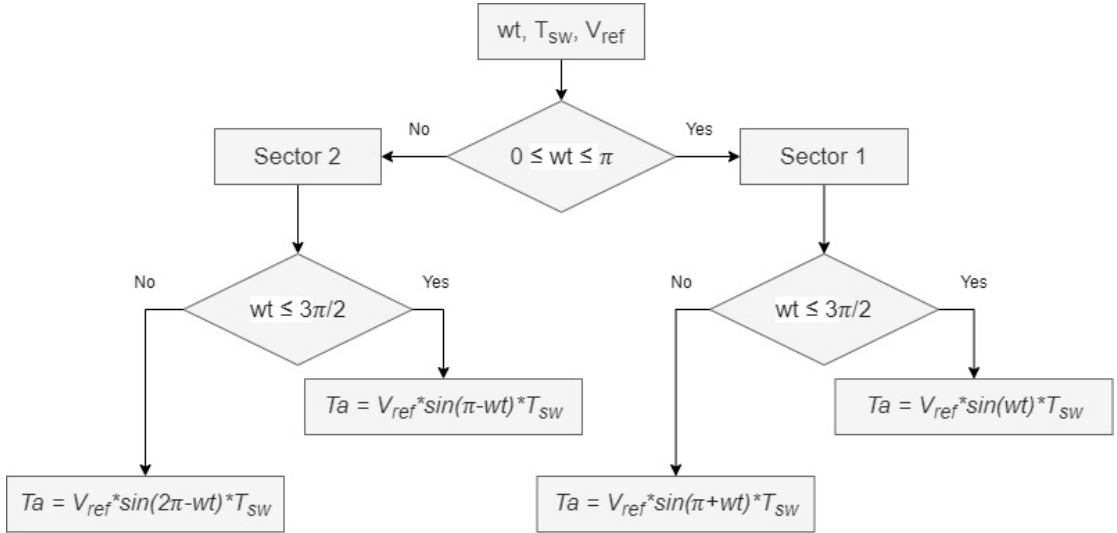


Figure 3.6: Single-phase Bipolar SVPWM flowchart.

3.10 Simulation

Full bridge inverter was simulated and tested on MATLAB/SIMULINK environment. Figure 3.7 - 3.12 are the schematic diagrams.

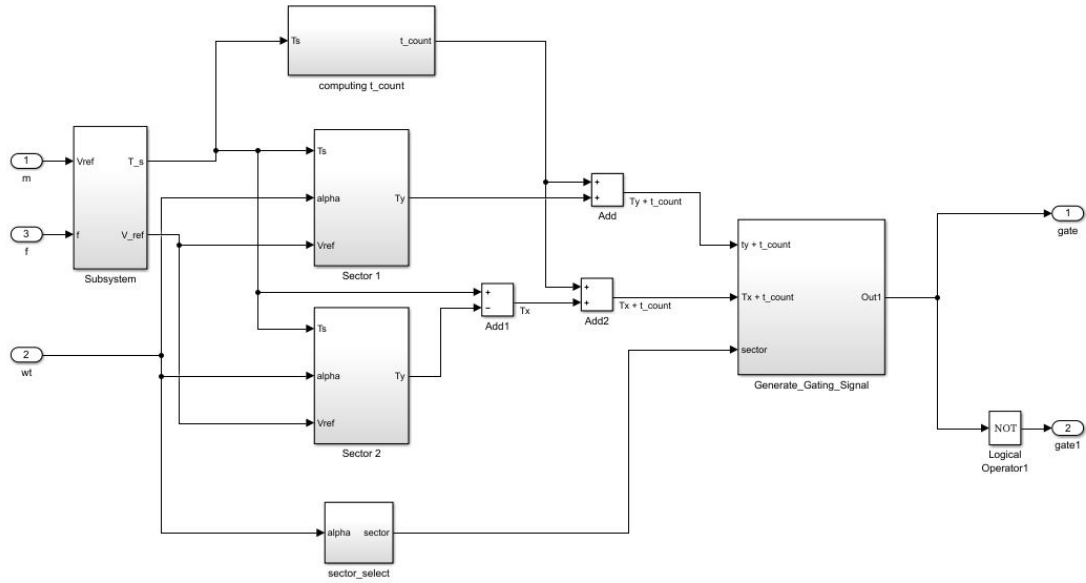


Figure 3.7: Block diagram of single phase SVPWM generator.

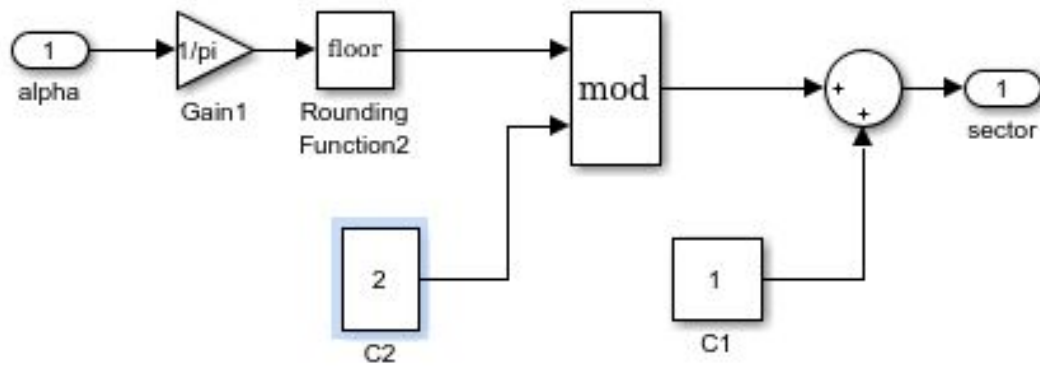


Figure 3.8: Sector selection.

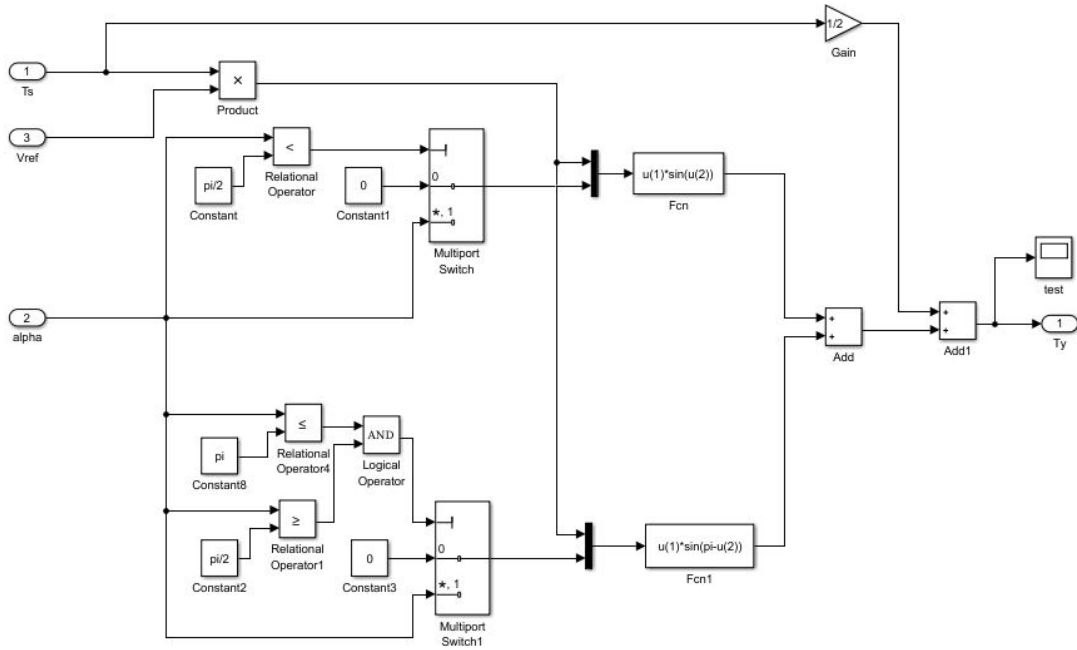


Figure 3.9: SVPWM Sector 1.

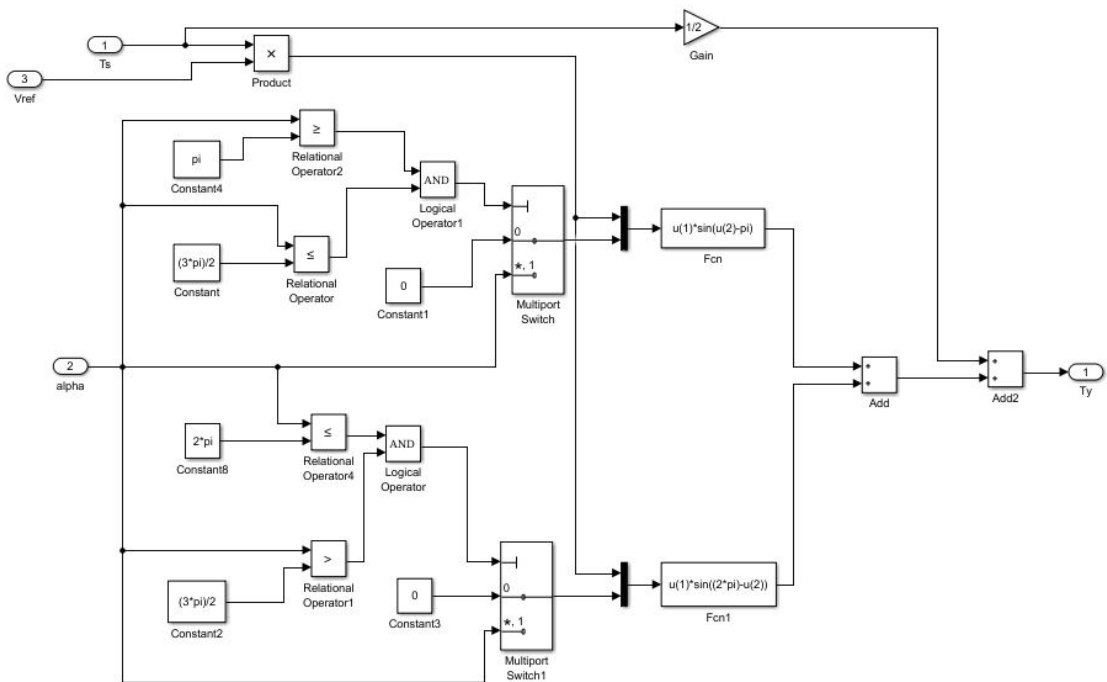


Figure 3.10: SVPWM Sector 2.

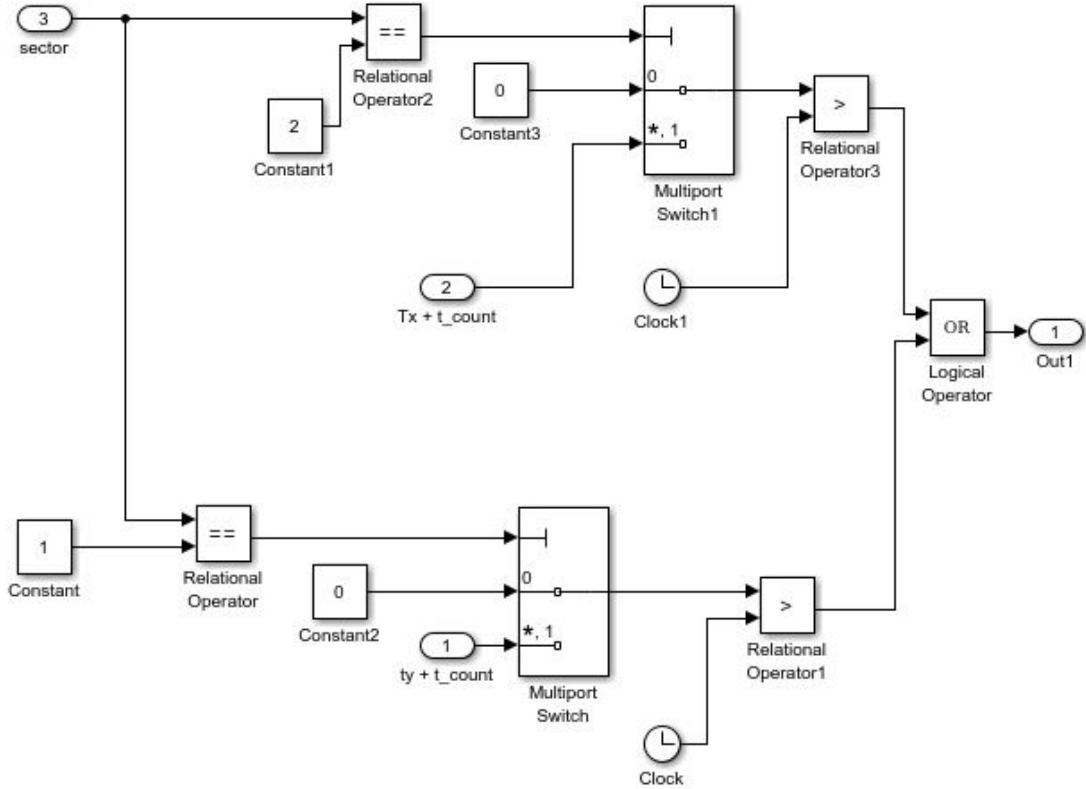


Figure 3.11: SVPWM generating gate signal.

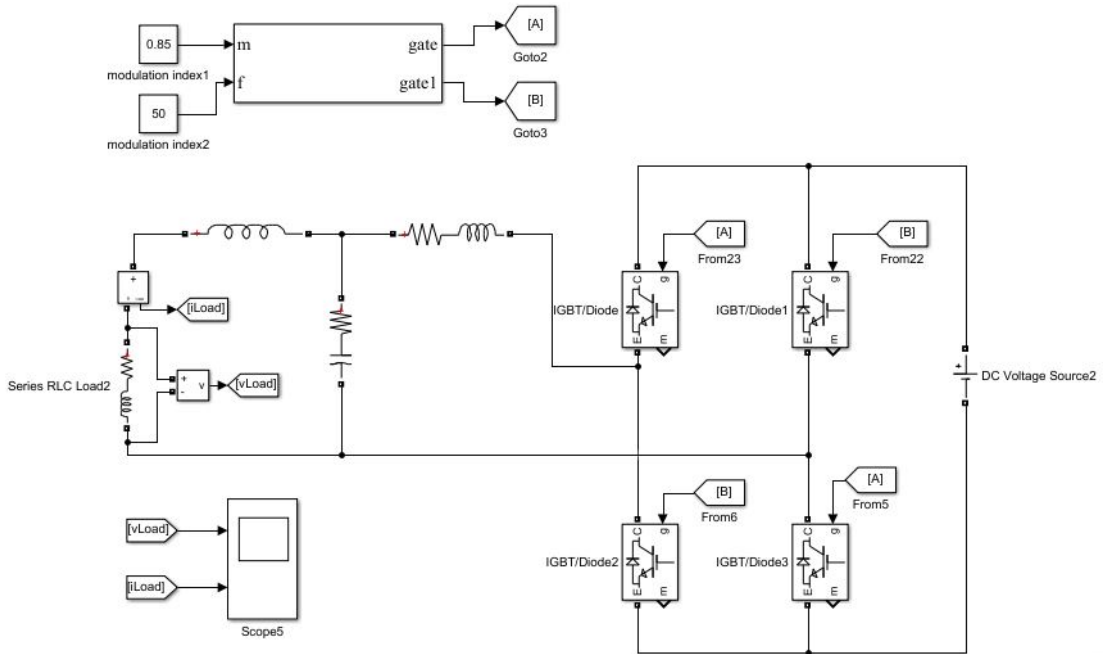


Figure 3.12: Full bridge single phase inverter with LCL filter.

4000W+500VAr load was connected with the full-bridge inverter. The generated SVPWM gating signal is shown in figure 3.13 and output voltage and current are shown in and 3.14

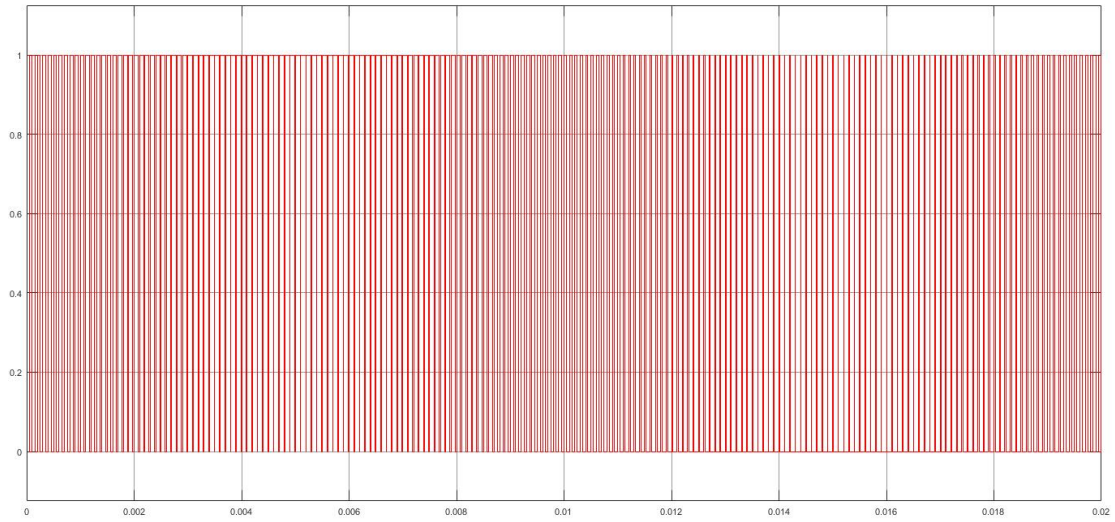


Figure 3.13: Generated SVPWM gating signal.

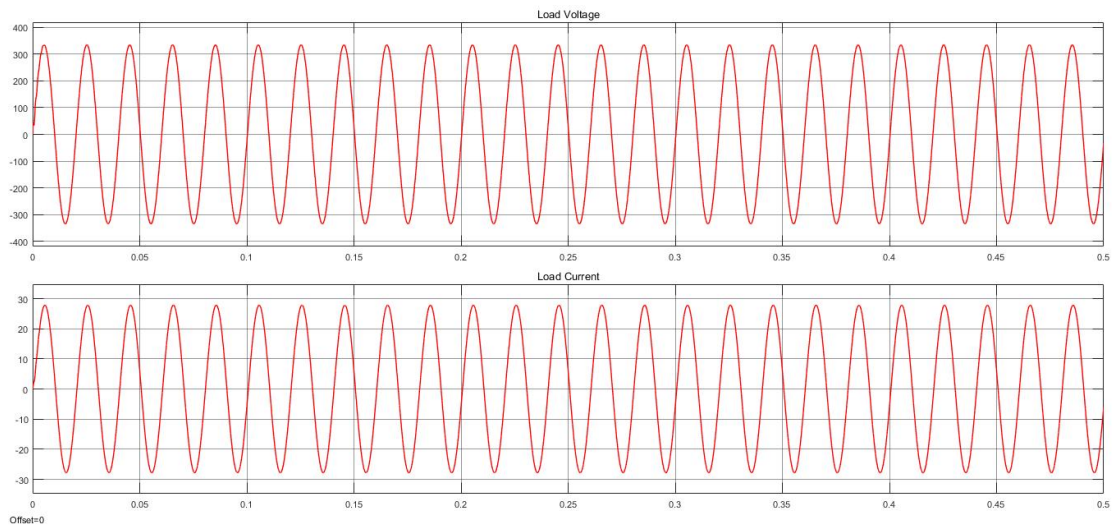


Figure 3.14: Output Voltage and Current of SVPWM based full bridge inverter.

Figure 3.15 shows the THD requirement filled according to the IEEE 516-2014 standards at full load.

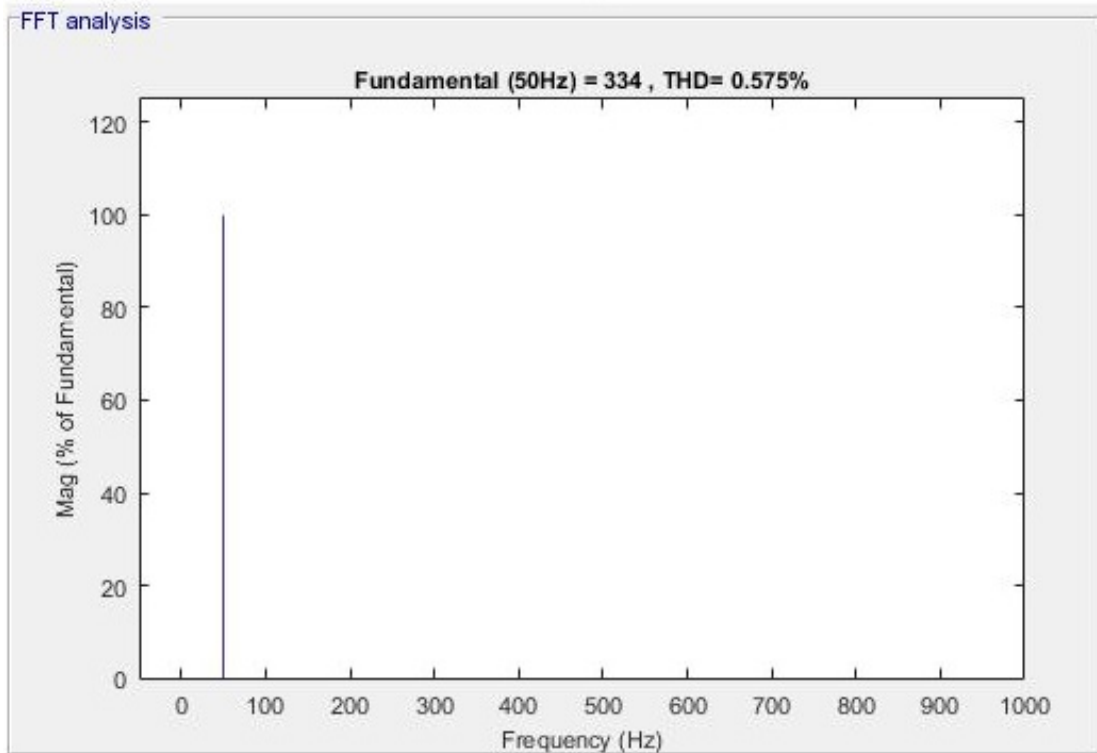


Figure 3.15: THD of SVPWM based full bridge inverter at Full Load.

Theoretical Aspects of Stationary and Synchronous Rotating Frame

4.1 Introduction

This chapter started with an explanation of the stationary reference frame, the synchronous rotating reference frame, and the transformations between these frames in a system of three phases. The Clarke transform [19, 24] is used to convert parameters within circuits to a two-dimensional stationary reference frame. The Clarke transformation is often used to translate balanced three-phase quantities into an orthogonal two-dimensional reference space, and is thus sometimes known as a 3-2 transform in that it transforms, for example three measured currents into two internal variables. The Park transform [24] three-phase electric machine models are the common examples of its application. It allows the elimination of time-variance of the parameter in the two-dimensional static reference frame by introducing a rotating reference frame, and referring the parameter to this. The Park transform is a 2-2 transform that also has a reference angle input. If the reference angle is rotating at the same speed as a frequency component of the two-dimensional input to the Park transform, the output of the latter corresponding to this frequency component will be time invariant.

This chapter evaluate the principles of the application of these transforms within a three-phase system, with a view to how they may be modified to apply to a single-phase system. Currently the transformation theories applications require at least two independent phases in the system. Therefore direct transformation from stationary to

rotating reference frame (the Park transform) is not possible in single phase inverters.

The end of this chapter provides an overview of the relevant published work for single-phase inverters. It discusses the single-phase inverters that currently employ the synchronous rotating frame controller, drawing on studies and previous research. This is aimed at understanding the limitations of such existing systems and identifying the direction the proposed development should take.

4.2 Synchronous and Reference Frames in Literature

In the 1920's, R. H. Park [24] restructured the analysis of electrical machines. Different types of variables were suggested in place of variables (currents, voltages, and flux) that are conventionally used in analysis of the stator windings of a synchronous machine these variables were similar to those concerning with the rotor. The unique property of Park's transformation emerged with eradicating all fundamental frequency components of time-varying parameters from the voltage equations of the synchronous machine that occur due to:

- Relative motion in the Electric circuits.
- The variation of magnetic reluctance in electric circuits.

Rotating induction electrical machines have the same basic principles in operation, but they differ from synchronous machines in the winding arrangement and the excitation method. Park's idea was developed by G. Kron [19] to deal with other types of rotating electrical machines. Consequently, each development in transformation was derived to analyze a type of rotating machine. There are several different forms of transformation depending on the reference frame chosen, such as stationary reference frame, synchronous reference frame, rotor reference frame, and arbitrary reference frame. However, in each of them, time variance of a synchronous machine is eliminated at the fundamental frequency by using the Park transform in which the reference frame is fixed in the rotor (or in the stator if this desired).

The process of transforming the three-phase system from the stationary frame to the synchronous rotating frame can be easily done by the following procedure:

1. Resolving the three-phases into two axes through the Clarke transformation as in 4.2.1. In other words, the three-phase stationary reference frame components are projected onto two orthogonal axes ($X\alpha$ and $X\beta$) appropriately fixed in the same stationary reference frame

$$\begin{bmatrix} X\alpha \\ X\beta \end{bmatrix} = \begin{bmatrix} 1 & -1/2 & -1/2 \\ 0 & \sqrt{3}/2 & -\sqrt{3}/2 \end{bmatrix} \begin{bmatrix} U \\ V \\ W \end{bmatrix} \quad (4.2.1)$$

Where U, V and W represent three-phase stationary-frame components, and $X\alpha$ and $X\beta$ represent the components projected onto the two stationary orthogonal axes.

$$\vec{r} = U \left(e^{j\theta} + e^{j(\theta+2\pi/3)} + e^{j(\theta+4\pi/3)} \right) \quad (4.2.2)$$

2. Transforming the two phase quantities ($X\alpha$ and $X\beta$) from the stationary reference frame to the synchronous rotating frame (with the corresponding d and q axes) that rotates with the rotor at an angular velocity (w) in the synchronous machine. This ensures that the synchronous rotating frame represents the stationary frame relative to the angular velocity of the system. In the case when these transformations apply to synchronous electrical machines, the key AC variables (voltage, current, and flux) become time-invariant at the fundamental frequency in the synchronously rotating reference frame. Equation 4.2.3 is known as the Park transformation, which performs the transformation from the stationary to the rotating reference frame axes (Xd and Xq)

$$\begin{bmatrix} Xd \\ Xq \end{bmatrix} = \begin{bmatrix} \cos wt & \sin wt \\ -\sin wt & \cos wt \end{bmatrix} \begin{bmatrix} X\alpha \\ X\beta \end{bmatrix} \quad (4.2.3)$$

Note that the Park transformation matrix is an orthogonal non-singular matrix ($T.T^{-1} = 1$). It represents the relationship between the stationary and rotating frame components.

These transformations lead to the new frame components becoming time invariant in the rotating reference frame rotating with angular velocity w .

The transformations and reference frame theory topic has recently received renewed interest in control strategies as a result of the following factors:

1. The time-invariant quantities (at the fundamental frequency) have advantages over time-variant quantities in the feedback control when compensated by using PI controllers. In other words, PI regulators gives considerably high steady state error in calculating amplitude and phase error, that's why they are considered poor performers when it comes to the control of AC systems.
2. Use of solid-state inverters for AC machine drives applications, in which transformation theory is already used for their control.
3. Digital controllers have become powerful, practical, and their cost has dropped rapidly. They are also popular in industry.
4. The design of voltage-source inverter switching strategies is most effectively done by using space vector pulse width modulation (SVPWM) [25].

4.3 Synchronous Frame Transformation in Three-Phase System

The rotating vector in the stationary reference frame becomes a constant vector in the rotating reference frame due to the rotation of the reference plane itself. Figure 4.1 shows stationary and rotating reference frame vector representations. The instantaneous angle θ is defined as

$$\theta = \int w(\tau) d\tau + \theta_{int} \quad (4.3.1)$$

Where w is the angular frequency in rad/sec, θ_{int} is the initial angle of the system, and τ is the time. In figure 4.1, \vec{X} is an arbitrary phase state variable projected into the stationary reference frame. It can be dissolved into two component vectors \vec{X}_α and \vec{X}_β ,

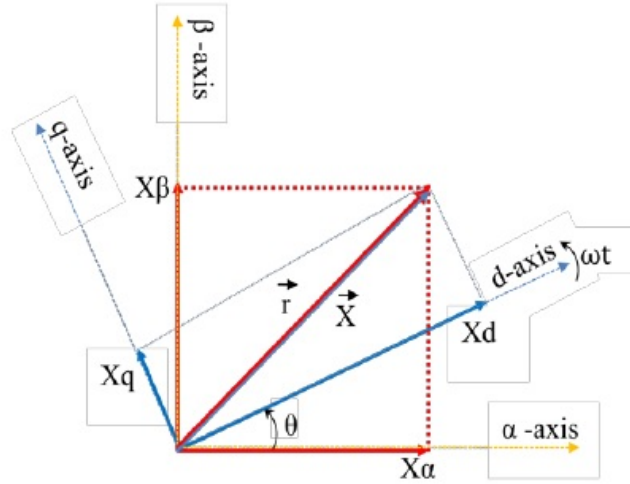


Figure 4.1: Clarke and Park transform in three phase system.

The rotating frame coordinate $(\vec{X}d, \vec{X}q)$ rotates in the same angular frequency and direction of \vec{X} . This leads to the magnitude of the rotating reference frame components being dependent on the magnitude of \vec{X} only, and not being affected by its instantaneous position in the stationary reference frame.

For more insight, let us consider $X\alpha$ and $X\beta$ representing the stationary reference frame components (of a voltage or current), and apply the Park transformation as in Eq 4.3.2,

$$\begin{bmatrix} Xd \\ Xq \end{bmatrix} = \begin{bmatrix} \cos wt & \sin wt \\ -\sin wt & \cos wt \end{bmatrix} \begin{bmatrix} X\alpha \\ X\beta \end{bmatrix} \quad (4.3.2)$$

where, $X\alpha = X \cos (wt + \phi)$ and $X\beta = X \sin (wt + \phi)$ and ϕ is the initial angle.

In AC electrical circuit the currents (the signal which is need to transformed) can lag their corresponding voltage by ϕ , while the transformation matrix is synchronous with the voltage waveform.

$$\begin{bmatrix} Xd \\ Xq \end{bmatrix} = \begin{bmatrix} \cos wt & \sin wt \\ -\sin wt & \cos wt \end{bmatrix} \begin{bmatrix} X \cos (wt + \phi) \\ X \sin (wt + \phi) \end{bmatrix} \quad (4.3.3)$$

$$\left. \begin{aligned} Xd &= \frac{X}{2} \{ [\cos (wt - wt - \phi) + \cos (wt + wt + \phi)] + [\cos (wt - wt - \phi) - \cos (wt + wt + \phi)] \} \\ Xq &= \frac{X}{2} \{ -[\sin (wt - wt - \phi) + \sin (wt + wt + \phi)] + [\sin (wt - wt - \phi) - \sin (wt + wt + \phi)] \} \end{aligned} \right\} \quad (4.3.4)$$

$$\left. \begin{aligned} Xd &= \frac{X}{2} \{ [\cos(-\phi) + \cos(2wt + \phi)] + [\cos(-\phi) - \cos(2wt + \phi)] \} \\ Xq &= \frac{X}{2} \{ [\sin(-\phi) - \sin(2wt + \phi)] + [\sin(-\phi) + \sin(2wt + \phi)] \} \end{aligned} \right\} \quad (4.3.5)$$

$$\left. \begin{aligned} Xd &= \frac{X}{2} [2\cos(-\phi)] \\ Xq &= \frac{X}{2} [2\sin(-\phi)] \end{aligned} \right\} \quad (4.3.6)$$

$$\left. \begin{aligned} Xd &= X\cos(-\phi) \\ Xq &= X\sin(-\phi) \end{aligned} \right\} \quad (4.3.7)$$

It is clear from eq. 4.3.7 that when the AC quantity represented by $(X\alpha, X\beta)$ is at sinusoidal steady-state, the rotating reference frame components Xd and Xq are constants (i.e. DC quantities). The rotating reference frame vector magnitude is dependent on the value of ϕ . When ϕ is equal to zero, Xd has a maximum value that is equal to X , and Xq is equal to zero.

4.4 Rotating Reference Frame Control Structure in Three-Phase Systems

Another method of structuring the control loop is by using a rotating reference frame. This method, also called d-q control, is extensively used in three-phase systems. Rotating reference frame regulators have become industry standard in the field of high-performance current-control methods. In this case, three-phase quantities (such as voltages, currents, etc.) are represented in terms of DC equivalent values or in other words, space vectors. Prompt variation of voltage and current in such model is valid, and this helped in sufficiently describing the system performance under both steady-state and transient operation [24]. In addition, it can offer ease of linking to the SVPWM technique of generating inverter switching states. Vector control is performed completely in the rotating d-q coordinate system to make the controller side elegant for a extremely vast range of applications, owing to its:

- Suitability for motor drive applications,
- Compatibility with the inverter gate-drive SVPWM technique.

- Flexibility to control grid-tied solid-state distributed generators.

Figure 4.2 represents the generic structure of the three-phase rotating reference frame control strategy.

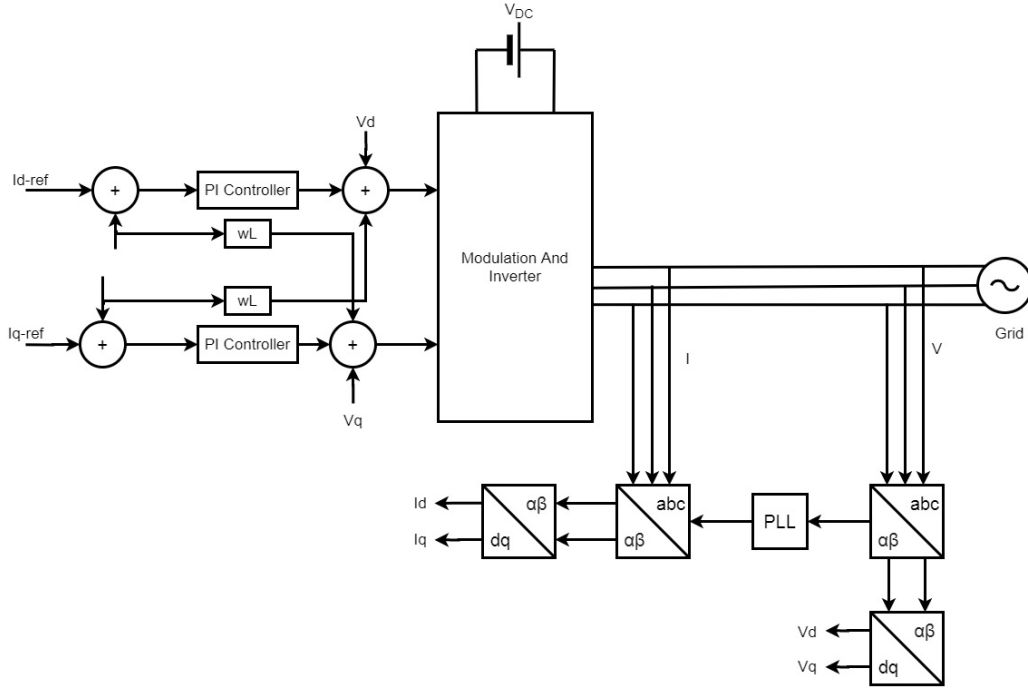


Figure 4.2: General structure of three-phase synchronous rotating reference frame control strategy.

In this method (synchronous rotating frame), the measured three-phase stationary current components are transformed to the two components ($\alpha - \beta$) by the Clarke transformation, which outputs a two-coordinate time-variant system (stationary system) through the mathematical representation shown in equation 4.2.1. In most cases, the three-phase system is symmetrical or balanced, which deduce that when the phases are summed their result is equal to zero. Thus, by transforming $\alpha - \beta$ from the stationary frame to the synchronous rotating frame (d-q) via Park transformation matrices, the d-q coordinates are arranged to rotate synchronously with the power line frequency (hence the term 'synchronous' rotating reference frame).

Some applications like in speed control of motor, variable voltage and frequency are require. In this case the inverter frequency may be simply defined by a voltage-controlled oscillator. The voltage value DC supply at the input of inverter is helpful in calculating the amplitude of output signal, however it can also be changed by controlling the inverter

switching circuit to provide a variable output voltage. In other cases, such as grid-tied inverters for renewable energy applications, the input DC supply is not consistent, hence the inverters are designed in a way that they provide desired output voltages regardless of the variation in DC input voltage. In such cases, they must deliver a fixed output voltage at a fixed frequency to the load since the application requires it and may depend on it. In this case, the output frequency is locked to that of the grid and is not variable by other means, e.g. by the user.

In the grid-tied inverter application, DC-to-DC converter regulates the value of DC-link voltage. This value is compared to the reference value of voltage and error is fed into the PI controller. The PI controller generates an output that is the required reference value of current vector. This vector decides the amount of active power that is provided at the output of inverter.

The other component of the current vector is the representative of reactive current. Its value can be manipulated to control the reactive power at the output of inverter. In other words, this component can be used to adjust the power factor. If reactive power is not desired to be injected, set the value of reactive current component to zero. But if the reactive power is required to be supplied (such as in power quality management), a non-zero reactive power reference can be used. The transformed d-q currents are sensed and then compared with their reference values, and the result is fed to the compensators to generate the feedback voltage references in the synchronous reference frame. The active and reactive power (or voltage) consists of a combination of feed-forward signals and decoupling of the inductive cross-coupling. These cross-coupling terms can be caused by the interaction between the inverter, filter circuit and PWM modulation scheme. The decoupling eliminates this coupling in the feedback controller between the d and q channels and yields two independent current controller channels. The voltage references are added to the feedback reference signal to form the total d and q axis voltage references. In the sinusoidal pulse width modulation (SPWM) technique, it is then necessary to transform from the d-q rotating frame variables to the $\alpha - \beta$ stationary frame variables. By inverse transformation from rotating synchronous frame to the stationary frame, the modulator can then generate the switching device gate signals. The phase angle is calculated from the grid voltage in order to match it with the phase of the controlled current. The synchronous reference frame regulator has many advantages for the three-phase grid-tied inverter:

- The control become time invariant and it provides fast response.
- Steady state error is achieved easily since controller mimics the design of conventional DC-DC converter.
- The attributes of the output voltage (i.e. Amplitude and phase) can be controlled separately. This helps in individual control of the active power and the reactive power
- Dynamic response is improved.
- Anti-islanding detection is improved [26–28]

The following matrix transfer functions shows the proportional-integral controller represented in the rotating synchronous reference frame.

$$G_{PI}^{dq} = \begin{bmatrix} Kp + Ki/s & 0 \\ 0 & Kp + Ki/s \end{bmatrix} \quad (4.4.1)$$

The synchronous rotating frame solves this problem by shifting fundamental power frequency information back to DC, at which point a conventional DC regulator can be used such as the PI controller. However, the synchronous-rotating-reference-frame controller is more complex in application.

4.5 Literature Review For Single-Phase Inverters Employing The Synchronous Rotating Frame Controller

The Clarke Transformation in single-phase inverter controller has been attempted and is discussed in [29–32]. The basic idea is to create an imaginary delayed signal, and use both of the signals together to create an orthogonal system as is usual in three-phase systems (Clarke Transformation).

Certain observations can be made from this, including some general observations relating to the transformation stage as well as the controller structure.

1. [29] discussed the generation of an orthogonal system by adding an imaginary signal delayed by a 1/4 cycle from original signal.

2. [33] shows the single-phase system transformation theory is not directly applicable, and additional complexity is needed for d-q transformations in the synchronous rotating reference frame.
3. It is difficult to implement synchronous rotating reference frame PI control using a digital signal processor (DSP) with fixed-point and low cost [34].
4. In the presence of an unbalanced load on a three-phase inverter, the quantities in the rotating reference frame are no longer completely time-invariant and contain a double line frequency component [32].
5. The harmonics associated with transformation stage come from using external sine and cosine functions in the transformation matrix. These functions are usually saved in a lookup table with limited precision [32].
6. The feedback signals are converted to the rotating frame and then transferred to the Controller stage in [29, 32]. Then, adding a transformation back to the stationary frame in order to apply PWM causes additional computational burden.

From the above reasons, use of the synchronous rotating reference frame lost its flavor in the single-phase inverter controller.

Control in DC-DC converters provide high dynamic response, the object of vector control is to obtain similar type of response. It is worth saying that it is too early to incorporate the voltage and current phase difference in the transformation stage. The transformation stages should be used for conditioning the feedback signal from time-variant to time-invariant only. This thesis validates SVPWM in single-phase inverter. Use of this method reduces additional computational burden caused by transformation back to the stationary frame before applying conventional PWM.

In a single-phase system, the harmonic terms at a frequency of $2w$ are a result from transformation stage itself. The $2w$ harmonic term can be a result for the following reasons:

- The created component is not orthogonal with the original component.
- The created and original components values are unequal.
- The coupling terms which are a result in transformation stage should be decoupled with opposite sign in controller stage.

Therefore, the progress in thesis is to mathematically model the power stage of a single-phase inverter that uses the theory of synchronous rotating reference frame mathematically. Then, solve the $2w$ harmonic issue and reduce computational requirements further.

4.6 Summary

Control in DC-DC converters provide high dynamic response, the objective of vector control is to obtain similar type of response. Hence, this chapter started by demonstrating synchronous rotating frame theory. In the later headings this chapter provides an overview of the published work that is relevant to single-phase inverters employing the synchronous rotating frame controller. It discusses the single-phase inverter controller, drawing on studies and previous research. Then, identifies the direction the proposed developments will take.

Single Phase Inverter Modeling Based on Synchronous Rotating Frame

5.1 Introduction

This begins starts with the state space modeling of inverter with LCL filter. later on it discusses the strategies to overcome difficulties in single-phase systems. One method that is suggested to create an orthogonal stationary component, similar to the one formed in Clarke transformation in three-phase systems. The system will then be in a position where the Park transformation can be applied in order to transition to a rotating reference frame.

The power stage of a voltage-source inverter designed for single-phase based based on the synchronous rotating reference frame is modelled mathematically. The principle of possible solutions is considered in and presented detail, ths incorporate the construction of the imaginary orthogonal circuit, stationary reference frame representation of the single-phase real circuit, and transformation of the single-phase stationary reference frame to the d-q rotating frame.

The aim is to build a single-phase inverter controller operating in the synchronous rotating frame which can produce high dynamic performance while being able to minimize error that is observed at the fundamental frequency, and thus to engance the quality of

electrical power quality generated by a single-phase inverter.

5.2 Single Phase Inverter Model

Consider a inverter filtering the output through LC filter is connected to the grid is given in 5.1. The inverter side Impedence is denoted as $L_i + R_i$, grid side impedance is $L_g + R_g$ and filter capacitor with resistance is given as $C_f + R_c$. Capasitor current is given as,

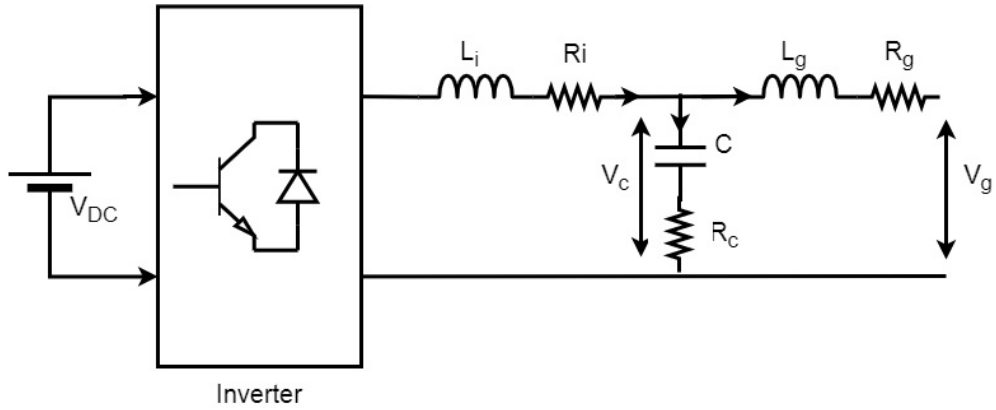


Figure 5.1: Single Phase Inverter Model with LCL filter.

Capacitor current is given by,

$$\begin{aligned}
 I_c &= I_i - I_g \\
 C_f \frac{dV_c}{dt} &= I_i - I_g \\
 \frac{dV_c}{dt} &= \frac{I_i - I_g}{C_f} \tag{5.2.1}
 \end{aligned}$$

Inverter side inductor voltage is given by,

$$\begin{aligned}
 V_{L_1} &= V_i - I_i R_i - V_c - I_c R_c \\
 L_i \frac{dI_i}{dt} &= V_i - I_i R_i - V_c - (I_i - I_g) R_c \\
 \frac{dI_i}{dt} &= \frac{1}{L_i} [V_i - I_i R_i - V_c - (I_i - I_g) R_c] \tag{5.2.2}
 \end{aligned}$$

Grid side inverter side inductor voltage is given by,

$$V_{L_2} = V_c + I_c R_f - I_g R_g - V_g$$

$$L_g \frac{dI_g}{dt} = V_c + I_c R_f - I_g R_g - V_g$$

$$\frac{dI_g}{dt} = \frac{1}{L_g} [V_c + I_c R_f - I_g R_g - V_g] \quad (5.2.3)$$

The state space model using equation 5.2.1, 5.2.2 and 5.2.3 can be written as,

$$\begin{bmatrix} \frac{dI_i}{dt} \\ \frac{dI_g}{dt} \\ \frac{dV_c}{dt} \end{bmatrix} = \begin{bmatrix} -\frac{(R_i+R_f)}{L_i} & \frac{R_f}{L_i} & -\frac{1}{L_i} \\ \frac{R_f}{L_g} & -\frac{(R_g+R_f)}{L_g} & \frac{1}{L_i} \\ \frac{1}{C_f} & -\frac{1}{C_f} & 0 \end{bmatrix} \begin{bmatrix} I_i \\ I_g \\ V_c \end{bmatrix} + \begin{bmatrix} \frac{1}{L_i} & 0 \\ 0 & \frac{1}{L_g} \\ 0 & 0 \end{bmatrix} \begin{bmatrix} V_i \\ V_g \end{bmatrix} \quad (5.2.4)$$

$$y = \begin{bmatrix} 1 & 0 & 0 \\ 0 & 1 & 0 \end{bmatrix} \begin{bmatrix} I_i \\ I_g \\ V_c \end{bmatrix} \quad (5.2.5)$$

5.3 Use of the Imaginary Orthogonal Phase in Single-Phase Systems

The d-q synchronous frame transformation method cannot be easily applied to single phase inverter due to the limitation of only one available phase. A method is to create a second orthogonal phase.

For introduction of additional imaginary phase in single phase inverter to constitute an orthogonal system analogous to Clark transform these approaches are discussed in literature.

1. A method is discussed in [35] to create orthogonal signal is by differentiating the output voltage of inverter and current of inductor. However this approach is highly sensitive to noise. Along with the fundamental component in the output voltage there are harmonics in the real phase of inverter. Differentiation process thus does not yield a purely orthogonal component. The inverter feedback controller is significantly affected by error in the stationary orthogonal phases. At the same time, the differentiation calculations require significant micro-controller processing time.
2. Another proposition is using an observer β -axis component[36]. This approach can achieve a good result, but it is very complex in terms of software and processing

requirements to design and implement. Hence, none of these approaches represents a solution that is simple or cheap to implement.

The approach adopted in this research is a technique to create an imaginary orthogonal phase, this is done by picking up the original signal and shifting its phase by 90° [29–31]. Using 5.3.1, the original phase delay of $1/4$ of the line phase of system can create another component (β) orthogonal with the original signal (α). The imaginary orthogonal component is estimated by picking up the real component, after introducing quarter cycle delay.

$$\begin{aligned} X_\alpha &= X \sin(\omega t) \\ X_\beta &= X \sin(\omega t - 90) \end{aligned} \tag{5.3.1}$$

The orthogonal stationary component (V_β) is created by a delay of 0.005 sec. Which make a $1/4$ th of the time period of 50Hz wave.

This method is examined using MATLAB/SIMULINK with input voltage $V_\alpha = 311 \sin(50 * 2\pi t)$. V_β is valid after 0.005 sec which represents a quarter-cycle delay from V_α . The process is to generate two stationary frames in a single-phase system in a way corresponding to the Clarke transformation in a three-phase system.

5.4 Modelling of the Single-Phase Inverter in Stationary and Rotating Reference Frames

A model for a single-phase inverter controller in the stationary and rotating reference frames was developed.

5.4.1 Single-Phase Inverter Model in Stationary Reference Frame

Figure 5.2 represents a real single-phase inverter scheme. The mathematical description is as follows,

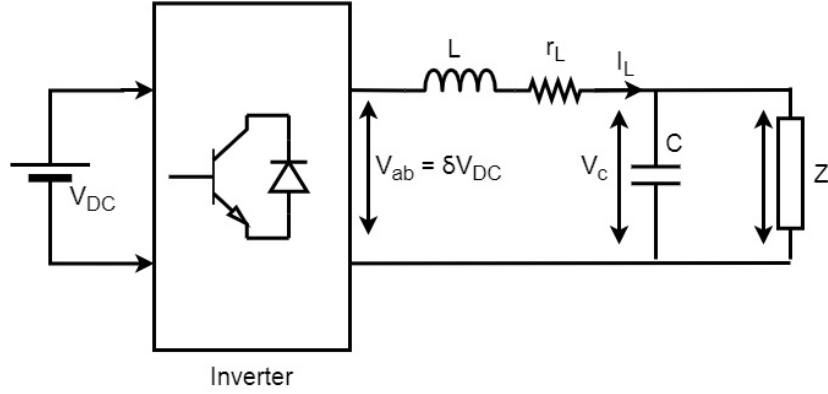


Figure 5.2: Single Phase Inverter Scheme.

$$L \frac{dI_L}{dt} + r_L I_L = V_{ab} - V_o \quad (5.4.1)$$

Where,

$$\delta = \begin{cases} 1 & v_{ab} = v_{DC} \\ 0 & v_{ab} = 0 \\ 1 & v_{ab} = -v_{DC} \end{cases} \quad (5.4.2)$$

$$I_L = C \frac{dv_c}{dt} + \frac{V_o}{Z} \quad (5.4.3)$$

Where δ is the duty cycle, Z is the combined impedance of load and L_g . A single-phase inverter average circuit model was developed by splitting the inverter model into two 'virtual' circuits as shown in figure 5.3. The imaginary circuit has a set of 'virtual' components with the exact same values as those in the real circuit. As the imaginary circuit does not exist practically, I_L is assumed and it is considered equal to the DC-link current (I_{DC}), this derivation is done from the real circuit for the purposes of modeling.

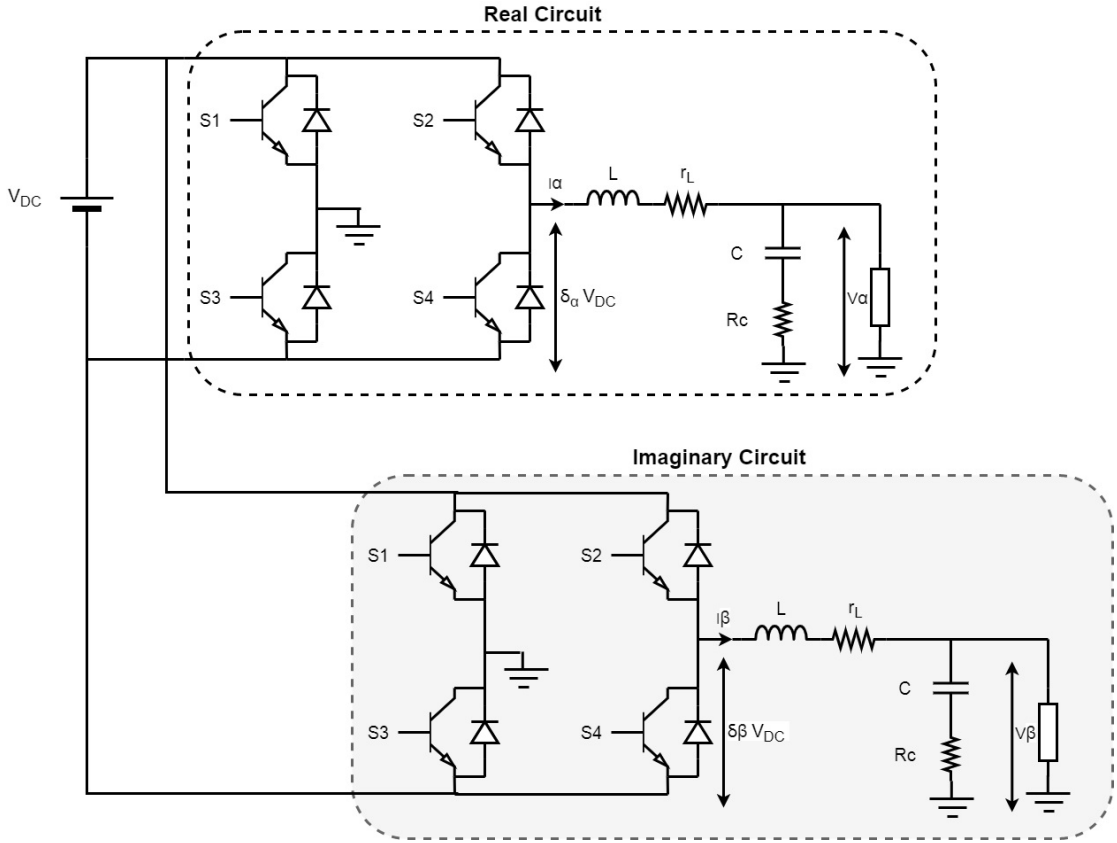


Figure 5.3: Single-phase inverter representation as real and imaginary parts of the circuit.

Rewriting the above equations using the real and imaginary circuits in Figure 5.3, the capacitor voltage and inductor current can be written as below:

$$\left. \begin{aligned} L \frac{dI_\alpha}{dt} + r_L I_\alpha &= V_{DC} \delta_\alpha - V_\alpha \\ L \frac{dI_\beta}{dt} + r_L I_\beta &= V_{DC} \delta_\beta - V_\beta \end{aligned} \right\} \quad (5.4.4)$$

$$\left. \begin{aligned} I_\alpha &= C \frac{dv_{\alpha C}}{dt} + \frac{V_\alpha}{Z} \\ I_\beta &= C \frac{dv_{\beta C}}{dt} + \frac{V_\beta}{Z} \end{aligned} \right\} \quad (5.4.5)$$

Where V_α is the real output voltage, V_β is the output voltage of imaginary circuit, I_α is the real inductor current, I_β is the imaginary inductor current.

The duty cycle (δ) can be averaged over one switching period providing that the highest frequency component in any change in $\hat{I}t$ does not violate the Nyquist criterion, it should be checked with respect to the switching frequency. Hence the dynamics of the system are constant over one switching period. The average filter voltage is obtained in 5.4.6.

$$\delta V_{DC} = \frac{1}{T_{sw}} v_{DC} \int_{t-T}^t \delta(\tau) d\tau = u \quad (5.4.6)$$

Where u is the inverter average sinusoidal duty ratio. Applying average state variables to the switching model of the single-phase inverter based on the real and imaginary circuits given in figure 5.3, equation 5.4.4 and 5.4.5 using equation 5.4.6.

$$\left. \begin{aligned} L \frac{dI_\alpha}{dt} + r_L I_\alpha &= u_\alpha - V_\alpha \\ L \frac{dI_\beta}{dt} + r_L I_\beta &= u_\beta - V_\beta \end{aligned} \right\} \quad (5.4.7)$$

$$\left. \begin{aligned} I_\alpha &= C \frac{dv_{\alpha C}}{dt} + \frac{V_\alpha}{Z} \\ I_\beta &= C \frac{dv_{\beta C}}{dt} + \frac{V_\beta}{Z} \end{aligned} \right\} \quad (5.4.8)$$

Where $v_{\alpha C}$ is the real capacitor voltage, $v_{\beta C}$ is the imaginary capacitor voltage.

$$\left. \begin{aligned} V_\alpha &= v_{\alpha C} + C \frac{dv_{\alpha C}}{dt} r_C \\ V_\beta &= v_{\beta C} + C \frac{dv_{\beta C}}{dt} r_C \end{aligned} \right\} \quad (5.4.9)$$

Substituting equation 5.4.9 in equation 5.4.7 and 5.4.8,

$$\left. \begin{aligned} L \frac{dI_\alpha}{dt} + r_L I_\alpha &= u_\alpha - [v_{\alpha C} + C \frac{dv_{\alpha C}}{dt} r_C] \\ L \frac{dI_\beta}{dt} + r_L I_\beta &= u_\beta - [v_{\beta C} + C \frac{dv_{\beta C}}{dt} r_C] \end{aligned} \right\} \quad (5.4.10)$$

$$\left. \begin{aligned} I_\alpha &= C \frac{dv_{\alpha C}}{dt} + \frac{1}{Z} [v_{\alpha C} + C \frac{dv_{\alpha C}}{dt} r_C] \\ I_\beta &= C \frac{dv_{\beta C}}{dt} + \frac{1}{Z} [v_{\beta C} + C \frac{dv_{\beta C}}{dt} r_C] \end{aligned} \right\} \quad (5.4.11)$$

As single-phase half-bridge inverter in real and imaginary stationary reference frames was considered in real and imaginary frames, its state-space average model is given in 5.4.12 and 5.4.13 and the circuit model is shown in figure 5.4.

$$\frac{d}{dt} \begin{bmatrix} I_\alpha \\ I_\beta \end{bmatrix} = \begin{bmatrix} u_\alpha \\ u_\beta \end{bmatrix} \frac{1}{L} \left(r_L + \frac{Z r_C}{Z + r_C} \right) - \begin{bmatrix} V_\alpha \\ V_\beta \end{bmatrix} \left(\frac{1}{L} - \frac{r_C}{L(Z + r_C)} \right) \quad (5.4.12)$$

$$\frac{d}{dt} \begin{bmatrix} v_{\alpha C} \\ v_{\beta C} \end{bmatrix} = \begin{bmatrix} I_{\alpha C} \\ I_{\beta C} \end{bmatrix} \frac{Z}{C(Z + r_C)} - \begin{bmatrix} V_{\alpha C} \\ V_{\beta C} \end{bmatrix} \frac{1}{C(Z + r_C)} \quad (5.4.13)$$

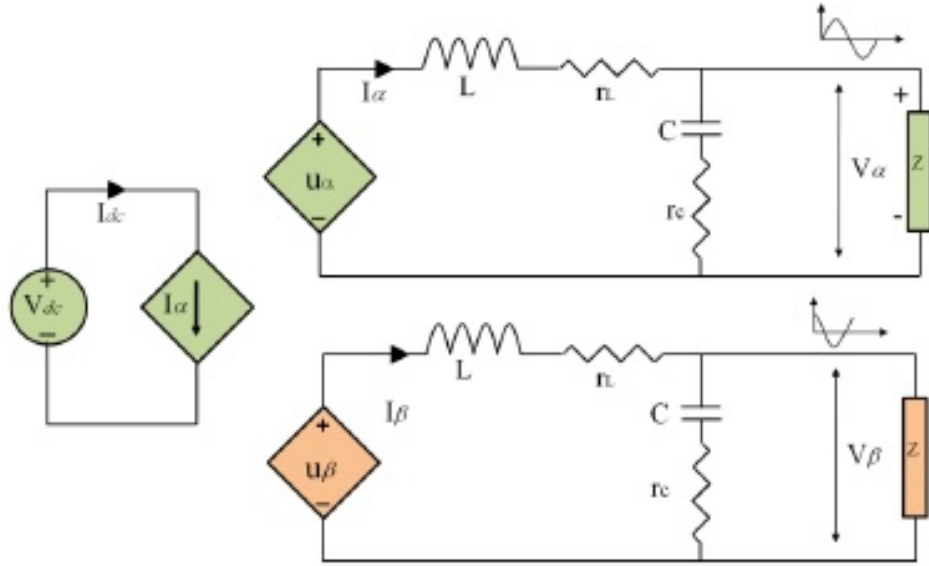


Figure 5.4: Stationary reference frames model of single-phase inverter.

In figure 5.4, symbols have the following meanings: Round symbol with internal +/- signs represents "constant voltage-source", diamond-shaped symbol with internal +/- signs represents "dependent voltage-source" with the dependency expression shown inside the symbol, diamond-shaped symbol with internal arrow represents "dependent current source" with the dependency expression shown inside the symbol.

5.4.2 Single-Phase Inverter Model in Rotating Reference Frame

Once the average real and the average imaginary models are obtained (as given in the equations 5.4.12 and 5.4.13, transformation matrix equation 5.4.14 and 5.4.15 can be applied to equations 5.4.12 and 5.4.13 if one want to achieve the d-q model of the inverter.

$$\begin{bmatrix} X_d \\ X_q \end{bmatrix} = T \begin{bmatrix} X_\alpha \\ X_\beta \end{bmatrix} \quad (5.4.14)$$

$$\begin{bmatrix} X_\alpha \\ X_\beta \end{bmatrix} = T^{-1} \begin{bmatrix} X_d \\ X_q \end{bmatrix} \quad (5.4.15)$$

Where (T) is transformation matrix.

$$T = \begin{bmatrix} \cos(\omega t) & \sin(\omega t) \\ -\sin(\omega t) & \cos(\omega t) \end{bmatrix} \quad (5.4.16)$$

$$T^{-1} = \begin{bmatrix} \cos(\omega t) & -\sin(\omega t) \\ \sin(\omega t) & \cos(\omega t) \end{bmatrix} \quad (5.4.17)$$

This results in 5.4.18 and 5.4.19:

$$\frac{d}{dt} \left(T^{-1} \begin{bmatrix} I_d \\ I_q \end{bmatrix} \right) = T^{-1} \begin{bmatrix} u_d \\ u_q \end{bmatrix} \frac{1}{L} - T^{-1} \begin{bmatrix} I_d \\ I_q \end{bmatrix} \left(\frac{r_L}{L} + \frac{r_C}{1 + r_C/Z} \right) - T^{-1} \begin{bmatrix} V_d \\ V_q \end{bmatrix} \left(\frac{1}{L} - \frac{1}{L(1 + r_C/Z)} \right) \quad (5.4.18)$$

$$\frac{d}{dt} \left(T^{-1} \begin{bmatrix} v_{dc} \\ v_{qc} \end{bmatrix} \right) = T^{-1} \begin{bmatrix} I_d \\ I_q \end{bmatrix} \left(\frac{1}{C(1 + r_c/Z)} \right) - T^{-1} \begin{bmatrix} V_{dc} \\ V_{qc} \end{bmatrix} \left(\frac{1}{ZC(1 + r_c/Z)} \right) \quad (5.4.19)$$

By applying the chain rule to the $\frac{d}{dt}(T^{-1} \begin{bmatrix} X_d \\ X_q \end{bmatrix})$ in equations 5.4.18 and 5.4.19, and separating d and q components, the state space model is obtained as given in 5.4.20 and 5.4.21, as follows

$$\frac{d}{dt} T^{-1} = \begin{bmatrix} -\omega \sin(\omega t) & -\omega \cos(\omega t) \\ -\omega \cos(\omega t) & -\omega \sin(\omega t) \end{bmatrix}$$

$$T \frac{d}{dt} T^{-1} = \omega \begin{bmatrix} -\cos(\omega t) \sin(\omega t) + \sin(\omega t) \cos(\omega t) & -(\cos(\omega t))^2 - (\sin(\omega t))^2 \\ (\sin(\omega t))^2 + (\cos(\omega t))^2 & -\cos(\omega t) \sin(\omega t) + \sin(\omega t) \cos(\omega t) \end{bmatrix}$$

$$T \frac{d}{dt} T^{-1} = \omega \begin{bmatrix} 0 & -1 \\ 1 & 0 \end{bmatrix} = \begin{bmatrix} 0 & -\omega \\ \omega & 0 \end{bmatrix}$$

$$\frac{d}{dt} \begin{bmatrix} I_d \\ I_q \end{bmatrix} = \begin{bmatrix} u_d \\ u_q \end{bmatrix} \frac{1}{L} + \begin{bmatrix} 0 & -\omega \\ \omega & 0 \end{bmatrix} \begin{bmatrix} I_d \\ I_q \end{bmatrix} - \begin{bmatrix} I_d \\ I_q \end{bmatrix} \left(\frac{r_L}{L} + \frac{r_C}{L(1 + r_C/Z)} \right) - \begin{bmatrix} V_d \\ V_q \end{bmatrix} \left(\frac{1}{L} - \frac{r_C}{LZ(1 + r_C/Z)} \right) \quad (5.4.20)$$

$$\frac{d}{dt} \begin{bmatrix} v_{dc} \\ v_{qc} \end{bmatrix} = \begin{bmatrix} I_d \\ I_q \end{bmatrix} \left(\frac{1}{C(1+r_C/Z)} \right) + \begin{bmatrix} 0 & -w \\ w & 0 \end{bmatrix} \begin{bmatrix} V_{dc} \\ V_{qc} \end{bmatrix} - \begin{bmatrix} V_{dc} \\ V_{qc} \end{bmatrix} \left(\frac{r_C}{CZ(1+r_C/z)} \right) \quad (5.4.21)$$

The d-q equations of inverter are simplified in 5.4.22 and 5.4.23 by neglecting r_C and as in practice they have very small values. D and q components of the system are presented. the cross coupling of terms can be observed in the equations mentioned below.

$$\frac{d}{dt} \begin{bmatrix} I_d \\ I_q \end{bmatrix} = \frac{1}{L} \begin{bmatrix} u_d \\ u_q \end{bmatrix} + \begin{bmatrix} 0 & -w \\ w & 0 \end{bmatrix} \begin{bmatrix} I_d \\ I_q \end{bmatrix} - \begin{bmatrix} I_d \\ I_q \end{bmatrix} \left(\frac{r_L}{L} \right) - \frac{1}{L} \begin{bmatrix} V_d \\ V_q \end{bmatrix} \quad (5.4.22)$$

$$\frac{d}{dt} \begin{bmatrix} V_d \\ V_q \end{bmatrix} = \frac{1}{C} \begin{bmatrix} I_d \\ I_q \end{bmatrix} + \begin{bmatrix} 0 & -w \\ w & 0 \end{bmatrix} \begin{bmatrix} V_d \\ V_q \end{bmatrix} - \frac{1}{CZ} \begin{bmatrix} V_d \\ V_q \end{bmatrix} \quad (5.4.23)$$

5.5 Double Feedback Loop Control Strategy

The control of inverter is adopts a double feedback loop control strategy. Out of the two loops the outer feedback loop is applied to the voltage and in the inner loop feedback is applied to the current [37]. Figure 5.5 shows a model of a single-phase voltage-source inverter. The structure of a two-loop controller is illustrated. The control system block diagram shows:

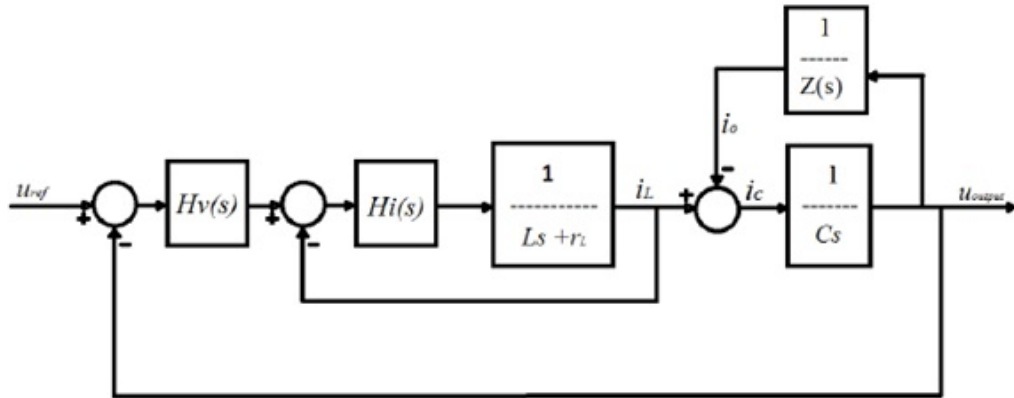


Figure 5.5: Controller structure with inner current loop and outer voltage loop.

- The inner loop uses the filter inductor current as a feedback signal, and $H_i(s)$ is the transfer function the inner loop PI controller.

- Load voltage is used in the outer loop as feedback signal, and $H_v(s)$ is the outer loop PI controller.

Where $H(s)$ represents the PI controller $H(s)=K_p+K_i/s$.

In order to generate the reference current for the inner loop, feed-forward controller is used, which is a PI controller acting on the DC supply voltage error, i.e. the difference between the DC voltage reference V_{DC_ref} and the measured DC voltage V_{bus} at the input of the inverter. The feed-forward controller is evident in the following blocks diagram of figure 5.6

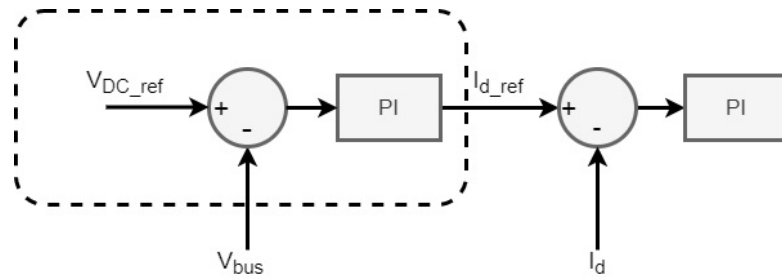


Figure 5.6: Feed-forward controller.

5.6 Grid-tied Inverter Mode

Alongside the stand-alone mode, renewable energy systems (RES) while powering household and business, can also operate in a grid connected mode. This allows the system to provide surplus energy to the utility grid or receive the power from the grid if the load is increased. Such energy systems are referred to as prosumers (producers and consumers). A net metering system is used in such scenarios where the difference between the produced and consumed power is calculated. The prosumer is charged if the energy is consumed or the amount is reimbursed if the power is supplied to the grid. 5.7 shows the grid-tied inverter circuit diagram in which the common coupling point is represented by node A.

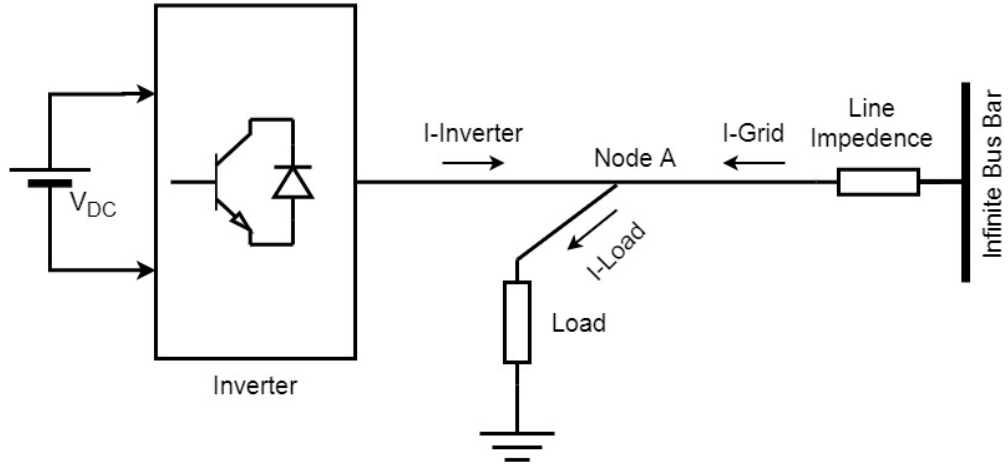


Figure 5.7: Grid tied inverter circuit diagram.

The single-phase voltage-source inverter and the grid are modelled in the synchronous rotating reference frame as two voltage-sources. The passive filter is placed between them, as shown in figure 5.8. The continuous-time state equation for the grid-tied inverter in the d-q coordinate system is,

$$u_d(t) = L \frac{di_d(t)}{dt} - \omega L i_q(t) + R i_d(t) + e_d(t) \quad (5.6.1)$$

$$u_q(t) = L \frac{di_q(t)}{dt} + \omega L i_d(t) + R i_q(t) + e_q(t) \quad (5.6.2)$$

Where $u_d(t)$ and $u_q(t)$ are the control signals components in the d-q frame respectively, $e_d(t)$ and $e_q(t)$ are grid voltage in the d-q frame respectively, R is equivalent line resistance, L is equivalent line inductance.

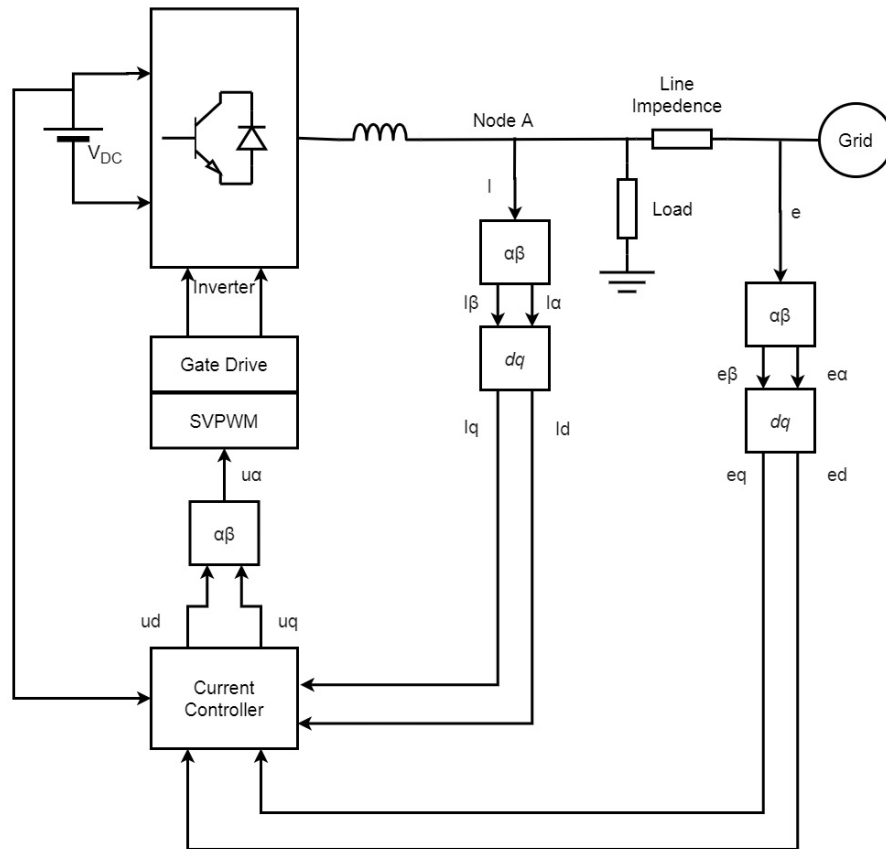


Figure 5.8: Grid tied inverter detailed circuit diagram.

5.7 Simulation and Results

The operation of single phase full bridge inverter connected with grid and variable load is shown in figure 5.9. Step increase of load from 2000W+225VAr to 4000W+225VAr at 0.1 sec and further increased to 5000W+225VAr at 0.2 sec is shown in figure 5.10.

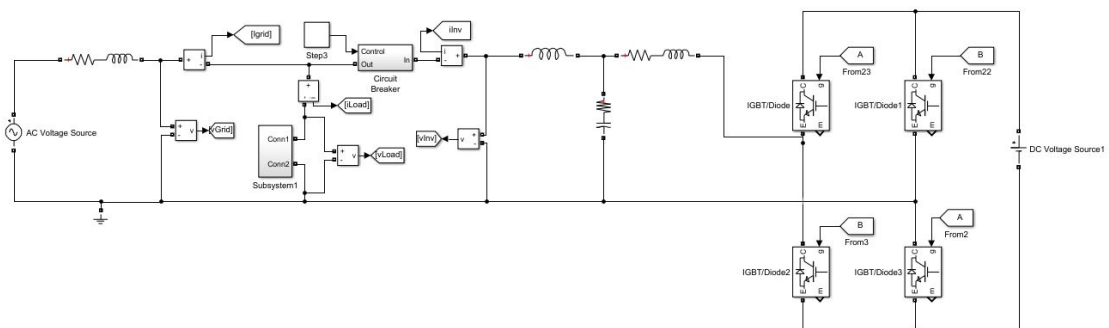


Figure 5.9: Full bridge inverter connected with grid and variable load.

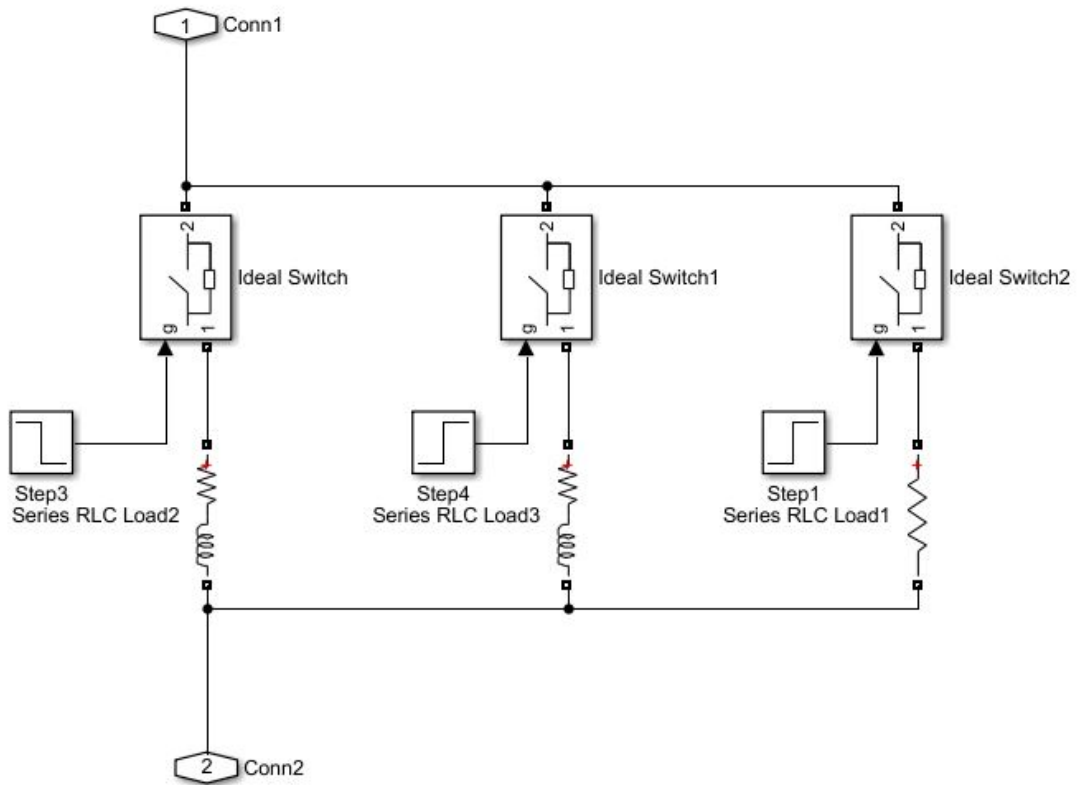


Figure 5.10: Step increase of load.

Figure 5.11 shows the conversion approach of current parameters from stationary reference frame to rotating reference frame. Same approach was used in conversion of voltage parameters.

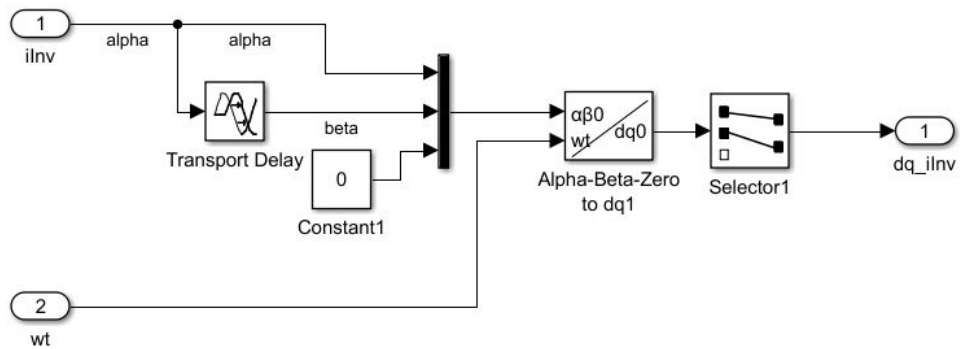


Figure 5.11: Alpha-Beta to DQ0 conversion.

Simulation diagram of current controller in synchronous rotating (DQ reference) frame is shown in figure 5.12.

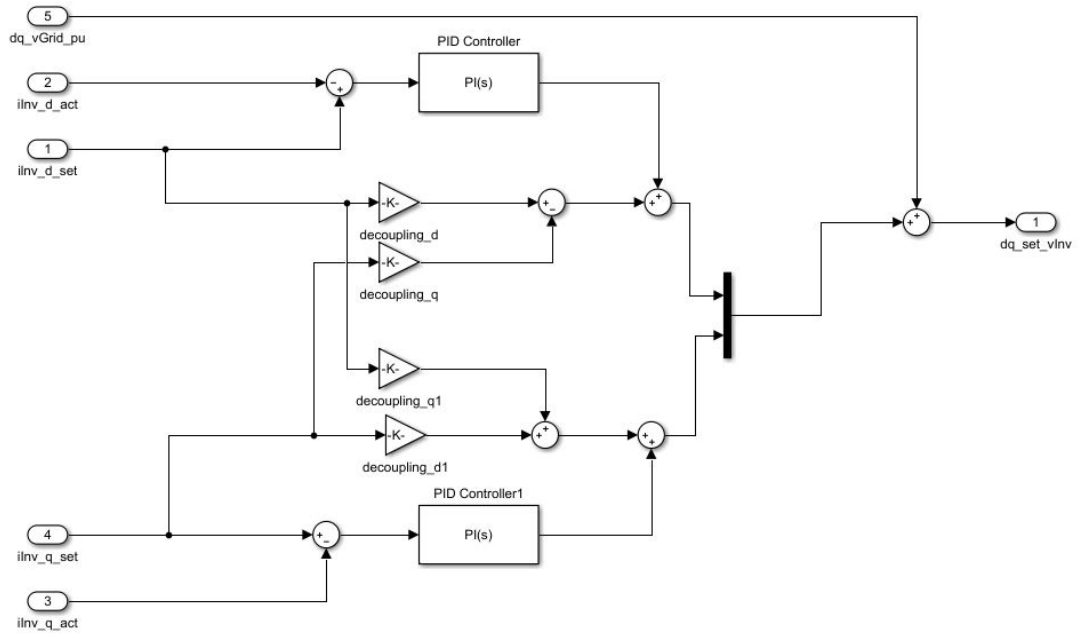


Figure 5.12: Current controller in DQ reference frame.

Figure 5.13 shows the behavior of inverter on different load demands. The conditions in inverter were set to provide maximum power i.e. 4500W. Initially 2000W+225VAr load was connected to the inverter. The inverter is providing current to the load and surplus current is injected into the grid it can be verified through the grid current which is out of phase from the inverter current. At 0.1sec the load was increased to 4000W+225VAr, inverter kept behaving as a primary source. The amount of current being injected into the grid decreased due to the increase in load demand. At 0.2sec the load demand increased beyond the capacity of load. At that time the grid take care of the increased demand and provide the excess current to the load.

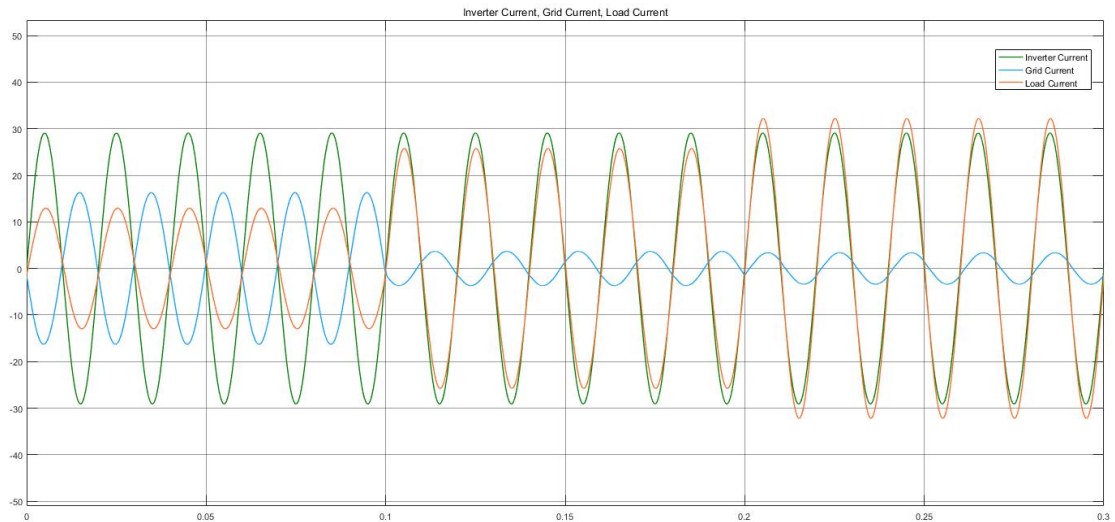


Figure 5.13: Current waveforms on increased load demand.

Figure 5.14 shows the common coupling point voltage and inverter current. It can be observed that variation in load does not affect the coupling point voltage of the inverter.

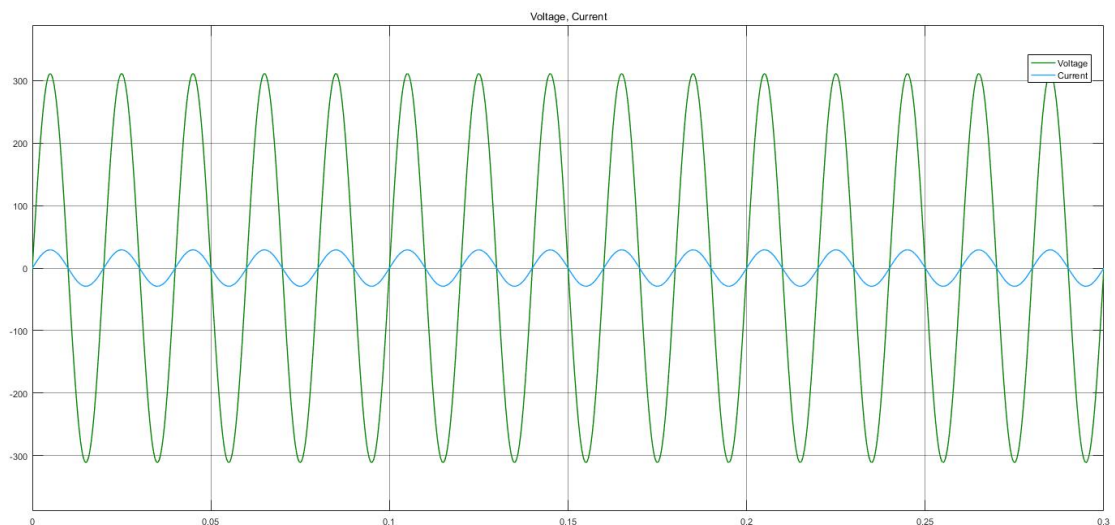


Figure 5.14: Coupling point Voltage and inverter Current.

5.8 Summary

This chapter shows the possible solutions to the problems of transformation to the synchronous rotating reference frame applied to a single-phase system. A single-phase inverter is modeled in the synchronous rotating reference frame has been accomplished,

including:

- Creating an imaginary circuit orthogonal to the real circuit.
- Converting the real circuit of single phase inverter into the stationary reference using real and imaginary orthogonal circuits.
- Transformation of the model in the single-phase stationary reference frame to the d-q rotating reference frame.

The transformation technique in the single-phase system is accomplished by the introduction of a phase delay of a quarter-cycle to the original phase. This action is adopted in order to generate two orthogonal components in the stationary reference frame in a manner analogous to the Clarke transformation in a three-phase system. Park transformation is then applied to generate the signals in synchronous rotating reference frame. In addition this chapter discusses the system performance and the control structure within the stand-alone inverter as well as in grid connect mode. The proposed transformation and control strategy offers certain advantages such as:

- The new transformation strategy overcomes the computational burden by using functions that are not computationally intensive. As a result, the system can be implemented with a low-cost fixed-point DSP.
- In [31, 36], the feedback signals are returned to the stationary frame in order to apply PWM. This creates additional computational burden. This study proposes SVPWM to avoid this step.

The proposed control strategy is able to operate with a stand-alone and grid connected inverter. It assumes the input DC-supply to inverter to be constant over one fundamental period of the power line frequency. For testing, the controller was exposed to transient conditions under a range of operational conditions, e.g. sudden load change, poor power factor load, nonlinear loads, with the load changes occurring under a range of resistive and inductive values. The dynamics of the system were examined at the instant of sudden load change to determine the transient response.

Finally, the single-phase voltage-source inverter and the grid are modelled in the synchronous rotating reference frame as two voltage-sources; the passive filter is placed

between them. This mode has two useful properties to be analyzed in the context of a grid-tied inverter:

1. Calculation or estimation of grid parameters at point of common coupling. these parameters include the amplitude and frequency of the grid voltage
2. Using these parameters apply a scheme like droop control to supply power (i.e. active and reactive, both independently) to the grid. This is to be discussed in the chapter 6.

Droop Control in Synchronous Solid-State Converter

6.1 Introduction

Small-scale individual power production from renewable energy is increasing day after day, leading to the decentralization of power generation. The power utilities now permit the placing of micro-generators on the customer side and the interfacing of them to the utility grid. Hence, the future of power network systems may largely be composed of a significant quantity of low-voltage renewable distributed generators interconnected through the distribution and transmission systems.

To achieve efficient and safe operation of the mentioned systems, it is crucial to understand the interaction between the generator and the utility. Therefore, this chapter offers a new technique to the implementation of decentralized embedded generators using synchronous solid-state inverters. Solutions are proposed for certain problems relating to the power management of single-phase solid-state power supplies as distributed generators using synchronous reference frame inverter control systems.

To prevent a generator from overloading when connected to the network, it is essential to ensure that the generator will share the load at a level proportional to its nominal power rating. This is achieved by adding extra control functions into the controller stage on the basis of voltage magnitude and frequency of each generator, known as droop control. Accordingly, an appropriate load sharing function was derived in order to enable this

new type of generator to contribute to the management of both active power and the reactive power within the network. Since the controller in the last chapter was designed in the rotating d-q reference frame and decouples active and the reactive power into separate channels, the load sharing function is designed in a way consistent with this approach.

6.2 Power Network Description

A traditional electrical power system is mainly composed of three separate parts [38, 39].

- Generation.
- Transmission.
- Distribution.

The generation stage is the first step in the power system, represented by a synchronous generator, where the terminal voltage is normally kept constant by field current regulation. The frequency is kept synchronous with the network frequency by regulating rotor speed. The equivalent circuit is represented by a voltage-source that is connected in series with a reactance. Larger power networks have smaller external impedances. Traditional power systems adopt centralized management concepts for distribution, demand and supply in a conventional top-down manner. At the production side the electrical energy is generated at a high voltage level and before reaching the consumer side, it is transformed down and distributed through several layers [38, 39]. This results in a rising cost associated with traditional centralized power systems in the production side as well as in the distribution and consumer side.

Most of the overhead distribution networks are low-voltage three-phase 4 wire systems. A distribution network has a number of low-voltage transformers with an output voltage (on the consumer side) of 230V or 400V that provide an acceptable level of losses. To maintain quality of the low-voltage network, the voltage magnitude and frequency must be compliant with the statutory limits. The statutory limits are recommended within most national standards. For example, International Electrotechnical Commission (IEC60038) provides the standard for 3-phase 4-wire LV systems, it suggest the

voltage variation within the limit $\pm 10\%$ of nominal voltage (a margin of -5% allowable voltage drops is included) [40].

In most cases, voltage and frequency controllers for solid-state power converters are designed to follow the load behavior. Many industrial applications require control of the instantaneous active and the reactive power values; in fact, they are used for managing power quality within their system. The Clarke and Park transformations are useful in three-phase solid-state inverter applications to study, analyze and control instantaneous active and the reactive powers. Control of the instantaneous active and the reactive power increases the stability margin, and improves the voltage regulation in three-phase solid-state inverter applications. The effectiveness of the instantaneous active and the reactive power control can be observed in the single-phase inverter application by using rotating reference frame theory [25, 41, 42].

6.3 Decentralized Power Management Concept

In brief the decentralized power management concept is how to generate a given amount of power distributed over smaller generators in a lot of places rather than a single generator in one place. This leads to the generation of electricity near the area of consumption. Consequently this allows more power to travel with less resistance to reach customers in rural as well as urban areas. One of the most valuable options is the theoretical capability to improve the continuity of power supply even with an upstream supply outage.

Where decentralized power supplies are permitted, the utilities allow the placing of numerous micro-sources interconnected with the distribution and transportation systems. In this case, as the number of micro-sources grows the power network will contain an increasing number of interdependent technologies and strategies, thus becoming more complex. A complex network can also be sparse over a large area. Therefore, many researchers have envisioned decentralized power supplies that do not require extensive communication with the central power stations.

Implementation of small-scale individual power production by renewable energy is increasing day after day. Thus, it is important to link these types of power production with the national power network. The network can then make optimal use of small-scale

energy generation, as well as allowing the use of renewable energy sources and facilitating operation in an autonomous grid-tied mode. Hence, the future power network systems could be composed of a large quantity of low-voltage renewable distributed generators.

On the other hand, there is a concern on the recent increase in the deployment of individual renewable energy generators within the national power network. This deployment represents a new type of distributed generation using power electronic inverters connected with the radial distribution network. Static inverters (i.e. not based upon rotating machines) have different properties when compared with conventional power plants based on rotating electromagnetic generators. To achieve safe and efficient integration of such inverters, it is necessary to develop decentralized control techniques at different levels for optimizing deployment of these new resources. Therefore, some requirement for regulation is needed for such resources in order that power quality does not worsen.

This research intends to explore the connection of single-phase inverters with a local network, and the solid-state inverter will appear as a distributed generator in this network. Hence, it is imperative to know the issues involved in controlling the inverter for ensuring both quality of supply and adequate supervision of power management.

6.4 Impact of Decentralized Distributed Generation on the Network

In hybrid applications, different types of energy sources (fuel, wind, solar, micro-turbine) work together. Since electricity cannot be stored in real-time in any major quantity, stability problems can be caused by mismatch between the supply and the demand. Network power quality depends on factors such as the types of distributed generators, capacity of distributed generators and the respective output power fluctuations, and the percentage of distributed generator types connected in this grid. The load is to be shared uniformly according to each generator's capacity.

Consequently, penetration of small-scale renewable energy distributed generators could have a significant impact on the power networks. To avoid large drops in the output voltage amplitude and frequency caused by load variations (through the grid-tied operation of distributed generators), each distributed generator's voltage amplitude and

phase need to be controlled so as to keep the network stable.

When such a distributed generator is grid-tied, the voltage and frequency of the common coupling point are dictated by the grid. Therefore, the distributed generator unit usually uses current control methods to deliver power to the network.

More questions are raised within the environment of decentralized solid-state distributed generators. Within the national network, a significant number of grid-tied small-scale individual renewable energy generators exist as distributed generators working in parallel. Synchronization is an issue that arises in this configuration. Synchronization is required to avoid currents circulating among the power sources and contributing to losses. Network estimators and phase lock loops allow the estimation of the grid frequency and phase at the common coupling point as well as the voltage magnitude.

Recently, for the grid-tied mode, load sharing based on droop methodology has been widely utilized for active and the reactive power control of electronically coupled three-phase distributed generator units. Three-phase power supplies were equipped with various droop control methods to provide continuous output average power.

Single-phase systems suffer from a characteristic of fluctuating output power. Thus far, little attention has been pushed to the dynamic properties and robustness of the grid-tied single-phase power supplies as distributed generators.

In the approach proposed in this thesis, a method that is based on the synchronous rotating frame within the controller stage (which is broadly similar to that used in three-phase inverters) was chosen. Droop control can be effective when used with such a system in grid-tied mode, subject to some means of communication between the converters being available.

6.5 Droop Function Methodology in Literature

In the droop control method, the distributed generator uses only locally-measured quantities at its common coupling point without extensive communications with other sources within the network. It is important to avoid generator overload, so the distributed generator controller must make sure that the component of the load power that is shared is within the normal power limit for the generator.

In this thesis, droop control has been chosen for controlling the inverter voltage mag-

nitude and its fundamental frequency during grid-tied inverter mode. This method is named differently in several papers depending on the approach applied [42–44].

New research uses the droop concept in different ways. Most work deals broadly with the problem [16]. [43] shows specifically the technical difficulty of power control when several subsystems work together such as energy sources, stored energy, power electronic inverters, grid and the loads. Other research [41] modifies the droop controller based on the line impedance parameters ratio (R/X), where R and X are the transmission line resistance and reactance respectively. This modification is suitable to the situations where the transmission line ratio (R/X) is high, such as in low-voltage rural applications. The line ratio (R/X) differs in each application depending on the line type and length used for connection with distributed generators.

The goal of all this work is to achieve a new decentralized distributed generator with the capability of operating in both isolated mode and to seamlessly connect to the utility (grid-tied mode). Important contributions concern the control of power electronic inverters operating as part of the power distribution network, as well as about power management.

It is a normal requirement to control output active and the reactive power of these types of distributed generators through inverter control. The inverter can adjust its response to the network and maintain voltage amplitude to meet the load demand.

The apparent power (S) flowing into network lines is described in figures 6.1 and 6.2 In a steady-state network operation the current flowing from voltage source $E(t)$ to $V_g(t)$ can be defines as,

$$I(t) = \frac{1}{(R + jX)}(E(t) - V_g(t)) \quad (6.5.1)$$

The active and the reactive power exported from the distributed generator to the grid can be expressed as follows,

$$S = P + jQ = E.I^* = \frac{E(E - V_g)}{Z} \quad (6.5.2)$$

Where S , P and Q are apparent, active and the reactive power, respectively, injected into the grid, E and V_g are the distributed generator and grid voltage magnitudes respectively, Z and θ are impedance magnitude and impedance angle, ϕ is the voltage

phase angle between the distributed generator and grid.

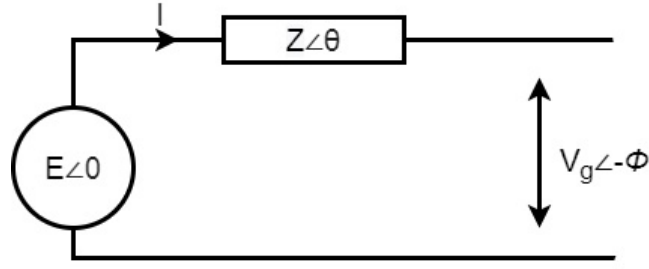


Figure 6.1: Network line power flow.

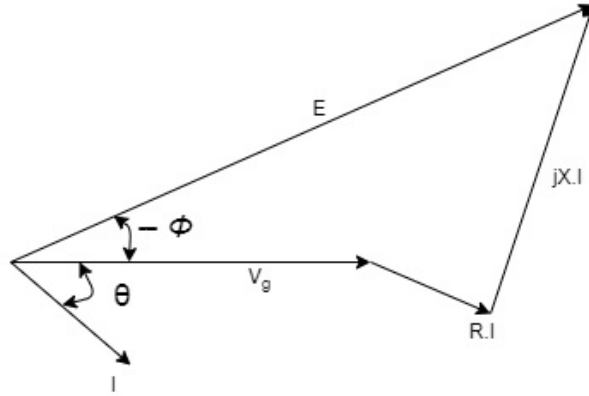


Figure 6.2: Line power flow phasor diagram.

The active and reactive is given as,

$$P = \frac{E^2}{Z} \cos\theta - \frac{EV_g}{Z} \cos(\theta + \phi) \quad (6.5.3)$$

$$Q = \frac{E^2}{Z} \sin\theta - \frac{EV_g}{Z} \sin(\theta + \phi) \quad (6.5.4)$$

where,

$$Ze^{j\theta} = R + jX \quad (6.5.5)$$

The equations 6.5.3 and 6.5.4 can be rewritten as:

$$P = \frac{E}{(R^2 + X^2)} [R(E - V_g \cos\phi) + XV_g \sin\phi] \quad (6.5.6)$$

$$Q = \frac{E}{(R^2 + X^2)} [R(E - V_g \sin\phi) + XV_g \cos\phi] \quad (6.5.7)$$

The simple concept of the droop method can be based on two assumptions:

1. The impedance in the overhead transmission lines is purely inductive, in other words $X \gg R$, and the resistance R can thus be neglected. Consequently $Z = X$ and $\theta + 90^\circ$. For the generators with low output impedance this approximation is valid. In the case when a solid-state distributed generator is used the instantaneous real and reactive power is exported to the network through a low pass filter to obtain the average active and reactive power. Consequently, the converter output impedance plays an important role in power sharing.

$$\sin\phi = \frac{XP}{EV_g} \quad (6.5.8)$$

$$E - V_g \cos\phi = \frac{XQ}{V_g} \quad (6.5.9)$$

2. The power angle ϕ is small, so $\sin\phi = \phi$ and $\cos\phi \approx 1$. Thus, equations 6.5.8 and 6.5.9 can be approximated as in equations 6.5.10 and 6.5.11

$$\phi \approx \frac{XP}{EV_g} \quad (6.5.10)$$

$$E - V_g \approx \frac{XQ}{V_g} \quad (6.5.11)$$

Equations 6.5.10 and 6.5.11 show that the voltage difference is proportional to the reactive power (Q), while the power angle is proportional to the active power (P) as expressed in 6.5.12

$$\left. \begin{aligned} \Delta P &\propto m(w_o - w) \\ \Delta Q &\propto m(E_o - E) \end{aligned} \right\} \quad (6.5.12)$$

Where ΔP and ΔQ are the generator active power and reactive slope respectively; w_o and E_o are the generator no-load frequency and voltage amplitude respectively; ω and v are the generator output frequency and voltage amplitude respectively,

thus, the active power is the function of frequency and it can be controlled by manipulating the frequency, and reactive power is function of voltage and it can be manipulated by controlling voltage magnitude. The above assumptions lead to two linear droop characteristics (P versus w) and (Q versus E), the droop functions are expressed in 6.5.13.

$$\left. \begin{aligned} w &= w_o - m(\Delta P) \\ E &= E_o - n(\Delta Q) \end{aligned} \right\} \quad (6.5.13)$$

Where m and n are droop slope coefficients (gains) according to their generator nominal power.

$$\left. \begin{aligned} m &= \frac{\Delta w}{P_{max}} \\ n &= \frac{\Delta E}{Q_{max}} \end{aligned} \right\} \quad (6.5.14)$$

Δw is maximum permissible variation in frequency and ΔE is maximum permissible voltage variation.

The droop characteristics of active power to frequency ($P - w$) and reactive power to voltage ($Q - E$) represent linear equations having fixed no-load values (w_o) and (E_o) respectively with the negative slopes. The droop characteristics in equation 6.5.13 are described in figure 6.3.

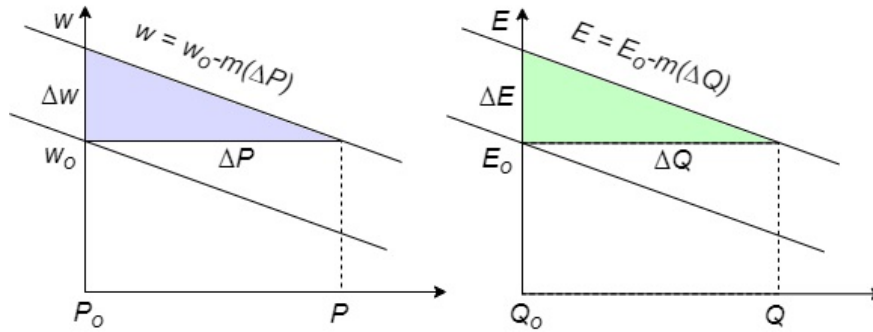


Figure 6.3: Droop curves for active and reactive power.

It is worth saying that the solid-state distributed generators will have a faster dynamic droop response than the rotating generators. The response of rotating generators is dependent on governor characteristics (e.g. inertia and torque). The distributed generators are synchronized to the network frequency at the point of common coupling. This

can be achieved by using a PLL or similar technique. Consequently, above equations 6.5.13 can be modified to use phase angle (ϕ) instead of frequency, as follows:

$$\left. \begin{aligned} \phi &= \phi_o - m(\Delta P) \\ E &= E_o - n(\Delta Q) \end{aligned} \right\} \quad (6.5.15)$$

[45] provided the interpretation (P - ϕ) and (Q - E) droop in terms of I_d and I_q . The voltage and current generated by the inverter can be transformed into DQ components resulting as,

$$E = \begin{bmatrix} E_d & E_q \end{bmatrix} \quad (6.5.16)$$

$$I = \begin{bmatrix} I_d & I_q \end{bmatrix} \quad (6.5.17)$$

Hence the power calculated in the DQ reference frame can be written as,

$$\begin{bmatrix} P \\ Q \end{bmatrix} = \begin{bmatrix} E_d & E_q \\ E_q & -E_d \end{bmatrix} \begin{bmatrix} I_d \\ I_q \end{bmatrix} \quad (6.5.18)$$

Since E is the reference putting value of $E_q = 0$ we get,

$$\begin{bmatrix} P \\ Q \end{bmatrix} = \begin{bmatrix} E_d I_d \\ -E_d I_q \end{bmatrix} \quad (6.5.19)$$

I_d tracks the active power of the distributed generator whereas ($-I_q$) tracks the reactive power of the distributed generator. Hence we can replace the conventionally used droop with the following equation, [45],

$$\left. \begin{aligned} \phi &= \phi_o - m(\Delta I_d) \\ E &= E_o + n(\Delta I_q) \end{aligned} \right\} \quad (6.5.20)$$

6.6 Simulation and Results

The control structure in this chapter was developed further to include the droop function. The control strategy of the grid voltage amplitude and the grid phase is based on

independent adjustment of the reactive and active power. The proposed control strategy was evaluated through MATLAB/SIMULINK in grid-tied mode. In order to test the steady-state and dynamic response during a load change, simulations were carried out with two types of possible operating conditions. The positive power value reveals the power exported to the node A, and vice versa. The system was tested in steps as follows:

- Case 1 - Constant power provided from inverter to variable load. Surplus power was injected into the grid
- Case 2 - Controlled the active and the reactive power provided from the inverter.

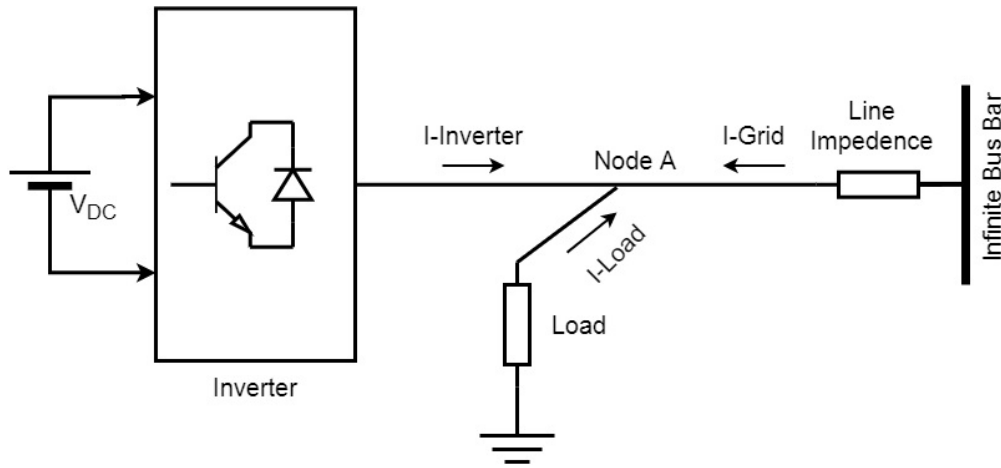


Figure 6.4: The inverter set to supply Active and Reactive Power ($S=P+Q$).

Case 1: The inverter was programmed to provide constant active and reactive power to regardless to the change in the load. In the test case inverter provided $4500W+500VAr$. Figure 6.5 show the result of simulation. Initially load was $6000W+750VAr$, the load was distributed between the grid and inverter. At 0.1sec the load decreased to $2500W+750VAr$, since the inverter provided the constant power, the surplus power from inverter was injected into grid. At 0.2sec load further decrease to $2000W+750VAr$. at 0.3sec the load further decrease to $500W$, all the reactive power from inverter was transferred into the grid while the active power was transferred into the load as well as grid.

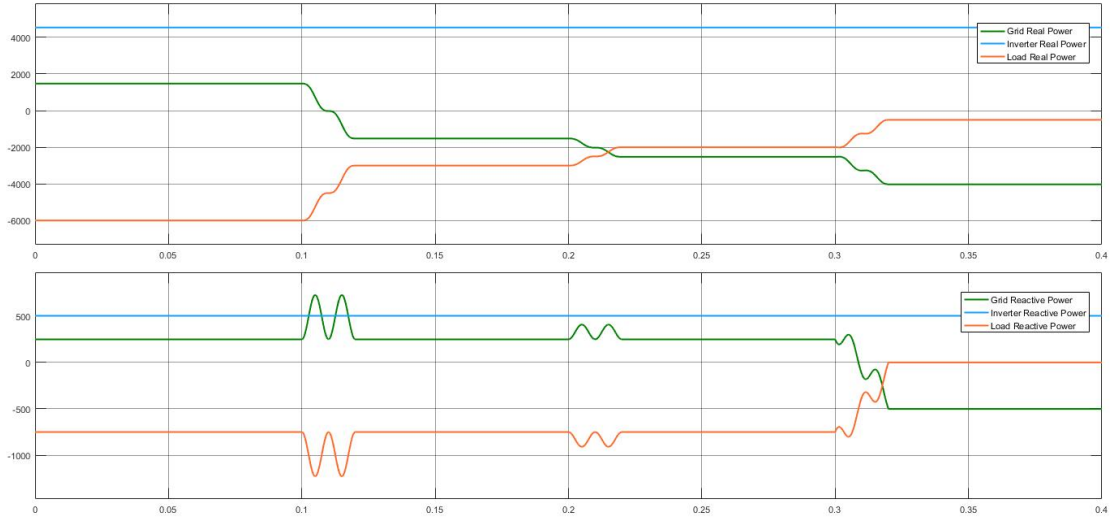


Figure 6.5: Constant power from inverter.

Case 2: Constant load was connect with the inverter while inverter was programmed to provide different values of active power and reactive power at particular instant, the simulation results are presented in 6.6. For the test case 3000W+1000VAR load was connected with the inverter. Initially inverter provided 4000W+1000VAR, surplus 1000W were injected into the grid, at 0.1sec inverter real power dropped to 1000W and no active or reactive power was transfered into the grid. At 0.2sec the power provided prom inverter further dropped to 2000W+500VAR, at that moment the input from grid came into action and provided the remaining 1000W+500VAR to the load.

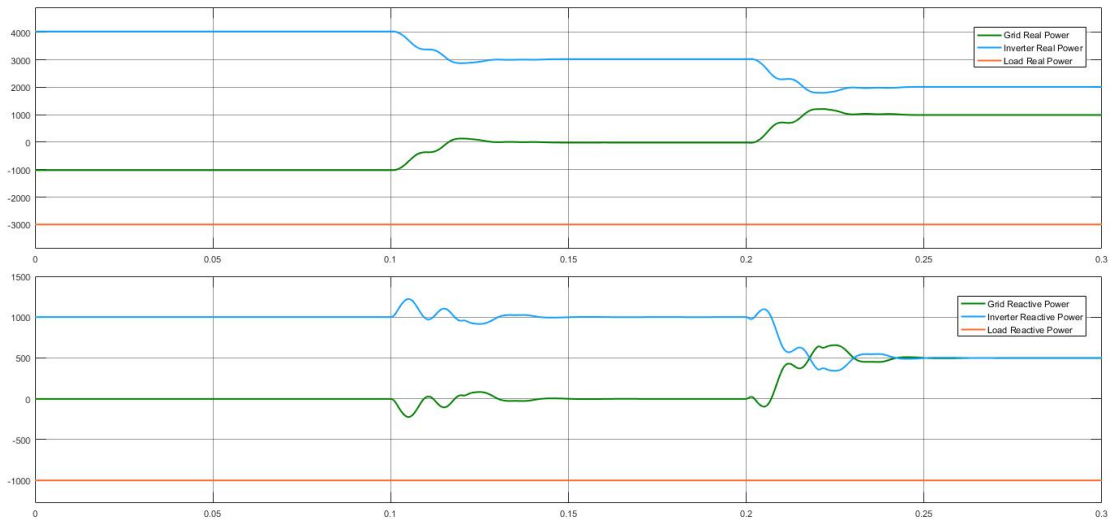


Figure 6.6: Variable power from inverter to constant load.

Conclusion and Future Work

7.1 Conclusion

This chapter summarizes and discusses the contributions made by this thesis and provides some suggestions for further research relating to the various topics considered. Techniques to develop novel and useful solutions for better connection between the distributed power generation systems and the utility network are considered. At the end, this chapter points out potential future work.

7.2 Summary

Inverters and their controllers are still undergoing development due to the fact that the requirements for inverter applications increase year upon year. Previous studies present many strategies of controller design that bring some advantages. With the advent of readily available high-speed embedded microprocessors and digital signal processors, the controller operating in the synchronous rotating reference frame has become the preferred solution for three-phase inverter applications in which high accuracy is required. However, a single-phase inverter controller design based on rotating reference frame theory has significant inherent complexity.

The transformation of AC waveforms to DC quantities through the use of a synchronous rotating reference frame is found to be a very useful tool for evaluating and designing controllers for three-phase inverters. The synchronous rotating reference frame controller has been proposed previously for high performance three-phase inverter applications.

This is due to the fact that time-invariant systems are easier to control than time-variant systems. After the transformation using the synchronous rotating reference frame, the internal representation of key signals becomes time-invariant. This:

- Provides a frequency transform such that the fundamental component of voltages at the power frequency is 'seen' as a time-invariant quantity, allowing the use of integral-term compensators (for example PI controllers) that are helpful in achieving steady-state error to be zero.
- Segregates the control of the phase offset and the amplitude into two separate channels.

In many cases, developments in single-phase systems have followed the developments in three-phase systems. Accordingly, this thesis proposes a type of synchronous rotating reference frame method for controlling single-phase inverters. Particular attention has been paid to the issues below:

1. Inverter modelling: Single-phase inverter modelling that is based on the synchronous rotating reference frame. As a result, the single-phase inverter model is represented as two parallel channels (Phase and Amplitude channels).
2. Feedback signal transformation (Clarke and Park transformations): Special attention was paid to achieve a transformation stage requiring limited computational complexity as well as resulting in harmonics sufficiently below 5%, it is satisfy the IEEE standard.
3. Controller structure: After the transformation step, the current and voltage feedback signals become time-invariant components separated in the 'phase' and the 'amplitude' channels. Each channel consists of two loops, a current loop that is the inner loop and outer loop that is voltage loop. This allows for an alternative implementation of a d-q controller. The proposed synchronous rotating frame controller yields enhancements in the applications of low-cost and high-performance single-phase inverters
4. Grid synchronization: This is based on a droop control technique. The inverter system is powered through DC batteries and due to their discharging cycles it can

supply power that is not constant with time. As a result, this static, solid-state type of generator differs in its properties to conventional rotating generators. The inclusion of this type of energy sources within the power distribution network will also promote the following two interests:

- Power quality improvement: the potential improvement in achievable power quality in terms of the total harmonic distortion, transient case at rapid load change, and transient case at sudden frequency change.
- Network enhancement: The overall security of the power network is enhanced by generating smaller amounts of power in a lot of places rather than a lot of power in one single place.

The converter presented in this thesis can perform in a 'flexible' grid-tied mode. This flexibility is achieved by managing the active and the reactive power that is injected to the grid from inverter at the common coupling point without requiring extensive communications between converters or the use of a centralized management service. The synchronous rotating frame technique for the single-phase inverter controller was developed in such a manner as to mimic synchronous rotating generators. Autonomous operation of inverters was achieved in form of droop control. The proposed control strategy allows for achieving P (real power) and Q (reactive power) regulation performance based on d-q rotating frame controller. The results demonstrate acceptable steady-state regulation and transient response.

5. Inverter switching gate-drive PWM technique: A part of the thesis has dealt with inverter switching gate drives by investigating the SVPWM algorithm for single-phase inverters. The newly developed SVPWM algorithm proposed herein is applicable to both single-phase half- and full-bridge inverters.

7.3 Future Work

The power conditioning unit proposed in this study focused a small-scale inverter system. Although a significant amount of research has been carried out in order to come up with the above-mentioned achievements and solutions, there is still place for more improvements.

1. This thesis proposes a low-cost controller strategy based on using a synchronous rotating reference frame that is capable of being implemented on platforms where computation speed is limited. This opens the door to enhance much previous work that is based on the synchronous rotating reference frame, for example multilevel converters and controlled rectifiers.
2. Further work to explore control of parallel-connected inverters can make use of the new transformation strategy. For instance, a peak current and/or average current controller could conceivably achieve good results when applied together with the new transformation strategy.
3. Paralleling of single-phase converters within a hybrid network is a good way to improve the power rating and system reliability.
4. The droop function used by the proposed controller can handle different transmission line R/X ratios and this subject can be studied further.

References

- [1] Muhammad H. Rashid. *Power Electronics, Devices, Circuits, and Applications, Fourth Edition*. Prentice Hall Inc., 2014.
- [2] J. J. Mendoza-Mendoza, J. C. Renteria-Soto, P. R. Martinez, G. Vazquez, G. Escobar, and J. M. Sosa. A comparative analysis of the 5l-ah6 and 5l-sc topologies for grid-connected transformer-less multilevel inverters for pv systems. In *2016 13th International Conference on Power Electronics (CIEP)*, pages 265–270, 2016.
- [3] Ieee recommended practice and requirements for harmonic control in electric power systems. *IEEE Std 519-2014 (Revision of IEEE Std 519-1992)*, pages 1–29, 2014.
- [4] E.Monmasson. *Power electronic converters; PWM strategies and current control techniques*. John Wiley & Sons., France, 2011.
- [5] M. El-Habrouk, M. K. Darwish, and P. Mehta. Active power filters: a review. *IEE Proceedings - Electric Power Applications*, 147(5):403–413, 2000.
- [6] H. Akagi. Active harmonic filters. *Proceedings of the IEEE*, 93(12):2128–2141, 2005.
- [7] M. Sanatkar-Chayjani and M. Monfared. Design of lcl and llcl filters for single-phase grid connected converters. *IET Power Electronics*, 9(9):1971–1978, 2016.
- [8] C. Cecati, A. Dell’Aquila, M. Liserre, and V. G. Monopoli. Design of h-bridge multilevel active rectifier for traction systems. *IEEE Transactions on Industry Applications*, 39(5):1541–1550, 2003.
- [9] S. Fukuda and R. Imamura. Application of a sinusoidal internal model to current control of three-phase utility-interface converters. *IEEE Transactions on Industrial Electronics*, 52(2):420–426, 2005.

REFERENCES

- [10] R. Chavali, A. Dey, and B. Das. Grid connected three-level vsi based smart solar inverter using online space vector based hysteresis current control. In *2020 IEEE International Conference on Power Electronics, Smart Grid and Renewable Energy (PESGRE2020)*, pages 1–6, 2020.
- [11] G. H. Bode and D. G. Holmes. Implementation of three level hysteresis current control for a single phase voltage source inverter. In *2000 IEEE 31st Annual Power Electronics Specialists Conference. Conference Proceedings (Cat. No.00CH37018)*, volume 1, pages 33–38 vol.1, 2000.
- [12] C. Yang, J. Wang, C. Wang, X. You, S. Yu, and P. Su. Tuning method of resonant current controller with dc elimination for pwm rectifiers in electric multiple units. *IEEE Transactions on Transportation Electrification*, pages 1–1, 2020.
- [13] S. A. Khajehoddin, M. Karimi-Ghartemani, P. K. Jain, and A. Bakhshai. A control design approach for three-phase grid-connected renewable energy resources. *IEEE Transactions on Sustainable Energy*, 2(4):423–432, 2011.
- [14] Qingrong Zeng and Liuchen Chang. Study of advanced current control strategies for three-phase grid-connected pwm inverters for distributed generation. In *Proceedings of 2005 IEEE Conference on Control Applications, 2005. CCA 2005.*, pages 1311–1316, 2005.
- [15] T. L. Vandoorn, B. Renders, L. Degroote, B. Meersman, and L. Vandevelde. Active load control in islanded microgrids based on the grid voltage. *IEEE Transactions on Smart Grid*, 2(1):139–151, 2011.
- [16] X. Wang, T. Liu, Y. Liu, and C. Zhang. Improved droop control strategy based on energy storage inverter in microgrid system. In *2019 IEEE 3rd International Electrical and Energy Conference (CIEEC)*, pages 1234–1239, 2019.
- [17] H. J. Avelar, W. A. Parreira, J. B. Vieira, L. C. G. de Freitas, and E. A. A. Coelho. A state equation model of a single-phase grid-connected inverter using a droop control scheme with extra phase shift control action. *IEEE Transactions on Industrial Electronics*, 59(3):1527–1537, 2012.
- [18] A. Reznik, M. G. Simões, A. Al-Durra, and S. M. Muyeen. *lcl* filter design and per-

REFERENCES

- formance analysis for grid-interconnected systems. *IEEE Transactions on Industry Applications*, 50(2):1225–1232, 2014.
- [19] G. Kron. *Equivalent circuits of electric machinery*. John Wiley and Sons, Inc., New York, 1951.
- [20] M. B. Booin and M. Cheraghi. Thd minimization in a five-phase five-level vsi using a novel svpwm technique. In *2019 10th International Power Electronics, Drive Systems and Technologies Conference (PEDSTC)*, pages 285–290, 2019.
- [21] G. Vivek, J. Biswas, M. D. Nair, and M. Barai. Simplified double switching svpwm implementation for three-level vsi. *The Journal of Engineering*, 2019(11):8257–8269, 2019.
- [22] V. Oleschuk and V. Ermuratskii. Review of methods and techniques of space-vector pwm for dual and triple inverters of pv systems. In *2019 International Conference on Electromechanical and Energy Systems (SIELMEN)*, pages 1–8, 2019.
- [23] P. Tripura, Y. Srinivasa Kishore Babu, and Y. Ravindranath Tagore. Space vector pulse width modulation schemes for two-level voltage source inverter. In *ACEEE Int. J. on Control System and Instrumentation*, volume 02, 2011.
- [24] P. C. Krause and O. Wasynczjk. Analysis of electric machinery [books and reports]. *IEEE Power Engineering Review*, 15(3):40–, 1995.
- [25] Y. Li and Y. W. Li. Decoupled power control for an inverter based low voltage microgrid in autonomous operation. In *2009 IEEE 6th International Power Electronics and Motion Control Conference*, pages 2490–2496, 2009.
- [26] X. Wang, W. Freitas, W. Xu, and V. Dinavahi. Impact of interface controls on the steady-state stability of inverter-based distributed generators. In *2007 IEEE Power Engineering Society General Meeting*, pages 1–4, 2007.
- [27] H. H. Zeineldin and S. Kennedy. Sandia frequency-shift parameter selection to eliminate nondetection zones. *IEEE Transactions on Power Delivery*, 24(1):486–487, 2009.
- [28] S. Kim, J. Jeon, and H. Choi. Design of dq-based voltage positive feedback for anti-islanding of a dg inverter. In *2009 Transmission Distribution Conference Exposition: Asia and Pacific*, pages 1–4, 2009.

REFERENCES

- [29] B. Crowhurst, E. F. El-Saadany, L. E. Chaar, and L. A. Lamont. Single-phase grid-tie inverter control using dq transform for active and reactive load power compensation. In *2010 IEEE International Conference on Power and Energy*, pages 489–494, 2010.
- [30] N. A. Ninad, L. A. C. Lopes, and A. Rufer. A vector controlled single-phase voltage source inverter with enhanced dynamic response. In *2010 IEEE International Symposium on Industrial Electronics*, pages 2891–2896, 2010.
- [31] S. Samerchur, S. Premrudeepreechacharn, Y. Kumsuwun, and K. Higuchi. Power control of single-phase voltage source inverter for grid-connected photovoltaic systems. In *2011 IEEE/PES Power Systems Conference and Exposition*, pages 1–6, 2011.
- [32] N. A. Ninad and L. A. C. Lopes. Per-phase dq control of a three-phase battery inverter in a diesel hybrid mini-grid supplying single-phase loads. In *2011 IEEE International Conference on Industrial Technology*, pages 204–209, 2011.
- [33] G. Shen, X. Zhu, J. Zhang, and D. Xu. A new feedback method for pr current control of lcl-filter-based grid-connected inverter. *IEEE Transactions on Industrial Electronics*, 57(6):2033–2041, 2010.
- [34] S. Yang, Q. Lei, F. Z. Peng, and Z. Qian. A robust control scheme for grid-connected voltage-source inverters. *IEEE Transactions on Industrial Electronics*, 58(1):202–212, 2011.
- [35] R. Carnieletto, D. B. Ramos, M. G. Simões, and F. A. Farret. Simulation and analysis of dq frame and p+resonant controls for voltage source inverter to distributed generation. In *2009 Brazilian Power Electronics Conference*, pages 104–109, 2009.
- [36] B. Saritha and P. A. Jankiraman. Observer based current control of single-phase inverter in dq rotating frame. In *2006 International Conference on Power Electronic, Drives and Energy Systems*, pages 1–5, 2006.
- [37] Bommegowda K.B, Vishwas K, Suryanarayana K, and N. M. Renukappa. Single phase inverter control with capacitor current feedback. In *2015 International Conference on Power and Advanced Control Engineering (ICPACE)*, pages 418–422, 2015.

REFERENCES

- [38] H. L. Willis and W. G. Scott. *Distributed Power Generation: Planning and Evaluation*. CRC Press, Ohio, United States, 2000.
- [39] S. Price K. E. Knapp, J. Martin and F. M. Gordon. Costing methodology for electric distribution system planning. *Prepared for the Energy Foundation*, 2000.
- [40] International standard (iec 60038:2009). *IEC standard voltages*, Edition 6.2, 2009.
- [41] J. Seo, H. Lee, W. Jung, and D. Won. Voltage control method using modified voltage droop control in lv distribution system. In *2009 Transmission Distribution Conference Exposition: Asia and Pacific*, pages 1–4, 2009.
- [42] R. S. Kushwah and G. R. Walke. Parallel operation of inverters with droop control of voltage and frequency. In *2018 International Conference on Smart City and Emerging Technology (ICSCET)*, pages 1–5, 2018.
- [43] T. Goya, E. Omine, Y. Kinjyo, T. Senjyu, A. Yona, N. Urasaki, and T. Funabashi. Frequency control in isolated island by using parallel operated battery systems applying hãŁd control theory based on droop characteristics. *IET Renewable Power Generation*, 5(2):160–166, 2011.
- [44] J. Seo, H. Lee, W. Jung, and D. Won. Voltage control method using modified voltage droop control in lv distribution system. In *2009 Transmission Distribution Conference Exposition: Asia and Pacific*, pages 1–4, 2009.
- [45] I. Alsaleh and L. Fan. Dq-axis current-based droop controller. In *2017 North American Power Symposium (NAPS)*, pages 1–6, 2017.